



TECHNISCHE  
UNIVERSITÄT  
WIEN  
Vienna | Austria

DISSERTATION

**THERMAL AND HYGRO-THERMAL PERFORMANCE  
EVALUATION OF AEROGEL CONTAINING PLASTER FOR RETROFIT  
OF HISTORIC BUILDINGS FAÇADES**

ausgeführt zum Zwecke der Erlangung des akademischen Grades  
eines Doktors der technischen Wissenschaften

unter der Leitung von  
Univ.-Prof. Dipl.-Ing. Dr. techn. Ardeshir Mahdavi  
E 259-3 Abteilung für Bauphysik und Bauökologie  
Institut für Architekturwissenschaften

eingereicht an der  
Technischen Universität Wien  
Fakultät für Architektur und Raumplanung

von  
Samira Aien  
Matr.Nr.: 1429960  
Bach Str.5, Ulm, Deutschland

Wien, Juli 2021

## ZUSAMMENFASSUNG

In den letzten Jahren haben sich viele Forscher auf die Energieeffizienz und Leistung bestehender Gebäude konzentriert. Um die hygro-thermische Leistung vorherzusagen und das Risiko von Feuchtigkeitsschäden in Nachrüstungsfällen zu minimieren, wurden benutzerfreundliche Feuchtigkeitsberechnungswerkzeuge entwickelt. Es wurden jedoch Bedenken geäußert, wie die Zuverlässigkeit solcher Werkzeuge erhöht werden kann. Angesichts der Auswirkungen des Klimas im Innen- und Außenbereich, der Anfangsbedingungen und der Lage der Isolierschicht sowie der Komplexität solcher Wechselwirkungen werden zunehmend komplexe Modelle der gleichzeitigen Wärme- und Feuchtigkeitsübertragung verwendet, um die Zuverlässigkeit von Gebäudeleistungssimulationen zu erhöhen.

Die vorliegende Studie verwendet Langzeitüberwachungsdaten und ein kalibriertes Gebäudesimulationsmodell, um eine Reihe bestehender und neuer Modelle unter Verwendung des Aerogels als Wärmedämmschicht zu testen. Um dieses Problem anzugehen, werden in der vorliegenden Studie langfristig überwachte Daten und ein kalibriertes Gebäudesimulationsmodell verwendet, um ein genaueres anfängliches Simulationsmodell sowie die Bewertung der Vorhersageleistung des Modells zu generieren. Die Modelle werden im Hinblick auf ihr Potenzial zur Vorhersage des thermischen und hygro-thermischen Verhaltens sowie auf ihre Wirksamkeit zur Verbesserung der Zuverlässigkeit von Simulationsbemühungen zur Gebäudeleistung bewertet. Darüber hinaus wurde der Einfluss der Position und Dicke von Aerogelputz auf die hygro-thermische Leistung von Wohngebäuden mithilfe eines kalibrierten Simulationsmodells untersucht. Generell kommt diese Dissertation zu dem Schluss, dass die korrekte Darstellung des lokalen Innen- und Außenklimas die Modellvorhersagen erheblich verbessern kann. Ebenso kann eine genaue Darstellung der Anfangsbedingungen (d. H. Startwerte der Schichttemperaturen und -feuchten) zu zuverlässigeren Simulationsergebnissen beitragen.

## SUMMARY

In recent years, many researchers have focused on the energy efficiency and performance of existing buildings. In order to predict the hygro-thermal performance and minimize the risk of moisture damage in retrofit cases, user-friendly moisture calculation tools have been developed. However, concerns have been raised as to how to increase the reliability of such tools. Given the impact of indoor and outdoor climatic, initial conditions and the location of the insulation layer and the complex nature of such interactions, complex models of simultaneous heat and humidity transfer are increasingly used to increase the reliability of building performance simulations.

The present study uses long-term monitored data and a calibrated building simulation model to test a number of existing and new models using the Aerogel as a thermal-moisture insulation layer. To address this issue, the present study deploys the data and calibrated models to generate a more accurate initial simulation model, as well as the evaluation of the predictive performance of the model. The models are evaluated in view of their potential in predicting thermal and hygro-thermal behavior, as well as their effectiveness to enhance the reliability of building performance simulation efforts. Moreover, it investigated the effect of aerogel plaster position and thickness on the hygro-thermal performance of residential buildings using a calibrated simulation model. In general terms, this dissertation concludes that the correct representation of the local indoor and outdoor climate can significantly improve model predictions. Likewise, accurate representation of initial conditions (i.e., starting values of layer temperatures and humidities) can contribute to more dependable simulation results.

## ACKNOWLEDGMENTS

First and foremost, I would like to express my sincere gratitude to my supervisor, Professor Ardeshir Mahdavi for his offered assistance and guidance at all levels of this work and for training me in this scientific field. His support and inspiring suggestions have been precious for the development of this thesis content.

My sincere thanks goes out to Professor. Matthias Schuss, for his continuous support and guidance throughout this research.

My center of gravity and my partner, Hamed, who knows me, always supports me and always motivates me and keeps me energetic during my dissertation.

From the bottom of my heart, I am grateful to my father, the greatest supporter of my life. A father whose life did not give him the opportunity to see this day and I will bear this regret for the rest of my life.

Last but by no means least, my deepest gratitude goes to my mother, brothers Saied and Vahid, my mother and father in-law who encouraged me with their love and support.

# TABLE OF CONTENTS

<b>CHAPTER 1. Introduction.....</b>	<b>1</b>
<b>1.1 Motivation.....</b>	<b>1</b>
<b>1.2 Background.....</b>	<b>2</b>
<b>1.3 Research Objectives .....</b>	<b>4</b>
<b>1.4 Structure of the Work .....</b>	<b>4</b>
<b>CHAPTER 2. General approach .....</b>	<b>6</b>
<b>2.1 Building Retrofit.....</b>	<b>6</b>
<b>2.2 Moisture control .....</b>	<b>7</b>
<b>2.3 Silica Aerogel.....</b>	<b>8</b>
2.3.1 Structure characterization.....	9
2.3.2 Gel preparation .....	10
2.3.3 Aging of the gel .....	10
2.3.4 Drying of the gel .....	11
2.3.5 Thermal conductivity.....	11
2.3.6 Acoustic properties .....	12
2.3.7 Safety and health aspects of aerogel .....	12
2.3.8 Building application of silica aerogel .....	14
<b>CHAPTER 3. Simultaneous Heat and Moisture Transport in Building Components .....</b>	<b>18</b>
<b>3.1 Introduction .....</b>	<b>18</b>
<b>3.2 Hygric effect on heat storage and transport.....</b>	<b>19</b>
3.2.1 Heat storage in moist building materials .....	19
3.2.2 Thermal conduction in moist building materials.....	20
<b>3.3 Heat and moisture transfer at building component boundaries</b>	<b>20</b>
<b>3.4 Assessment of the calculation method .....</b>	<b>21</b>
3.4.1 New calculation techniques and functional characteristics ..	21
3.4.2 Hygro-thermal assessment.....	23
3.4.3 Accuracy of risk assessment methods .....	23

3.4.4	The Glaser method .....	24
3.4.5	The WUFI calculation method .....	24
<b>CHAPTER 4.</b>	<b>heat and moisture model calibration .....</b>	<b>26</b>
<b>4.1</b>	<b>Introduction .....</b>	<b>26</b>
<b>4.2</b>	<b>Methodology .....</b>	<b>26</b>
<b>4.3</b>	<b>Case Study Building .....</b>	<b>27</b>
4.3.1	Monitoring data .....	32
4.3.2	Long-term evaluation of aerogel plaster with various finishings 34	
4.3.3	Hypro thermal simulation with WUFI Pro and WUF 2D .....	42
4.3.4	Program Setting and Inputs .....	43
4.3.5	Boundary Conditions .....	44
4.3.6	Sensitivity Analysis .....	46
4.3.7	Calibration .....	54
<b>4.4</b>	<b>Evaluation Method .....</b>	<b>56</b>
<b>4.5</b>	<b>Result and Discussion .....</b>	<b>56</b>
<b>CHAPTER 5.</b>	<b>Evaluation of thickness and location of insulation layer in wall configuration .....</b>	<b>66</b>
5.1.1	Case Study .....	67
5.1.2	Simulation Tool .....	69
5.1.3	Simulation scenarios .....	69
5.1.4	Performance criteria .....	71
5.1.5	Result and discussion .....	72
<b>CHAPTER 6.</b>	<b>Conclusion .....</b>	<b>76</b>
<b>6.1</b>	<b>Contributions .....</b>	<b>76</b>
<b>6.2</b>	<b>Future Research .....</b>	<b>77</b>
<b>CHAPTER 7.</b>	<b>Reference .....</b>	<b>78</b>
<b>7.1</b>	<b>LITERATURE .....</b>	<b>78</b>
<b>7.2</b>	<b>List of tables .....</b>	<b>86</b>
<b>7.3</b>	<b>List of equations .....</b>	<b>87</b>

<b>7.4</b>	<b>List of figures.....</b>	<b>88</b>
<b>7.5</b>	<b>Building Matrix.....</b>	<b>91</b>
<b>7.6</b>	<b>Documentation of a building in Habichergasse 20, Vienna .....</b>	<b>93</b>
7.6.1	Vertical sections of a building in Habichergasse 20, Vienna .	93
7.6.2	Facades of a building in Habichergasse 20, Vienna .....	94
7.6.3	Roof plan of a building in Habichergasse 20, Vienna .....	94
7.6.4	Plan of the first floor of a buiding in Habichergasse 20, Vienna	95

# CHAPTER 1.

## INTRODUCTION

### 1.1 Motivation

Fossil fuels are the largest non-renewable energy resources that they emissions CO<sub>2</sub> and greenhouse gasses when they burn, which contributes to increases global warming. The biggest energy demand in Europa are heating and cooling about 84% which, they are generated from fossil fuels and it is expected to remain so (European Commission 2016). According to the Directive 2012/27/EU ([Http://www.buildup.eu/en](http://www.buildup.eu/en), n.d.), based on the conclusions lead by the Council on the Energy Efficiency Plan 2011, the construction sector causes 40% of the energy consumption. Building sector is responsible for one-third of global greenhouse gas emissions annually via consuming of heating and cooling energy (Ürge-Vorsatz et al. 2015). In Europe, 9 billion square meters of the residential stock have been built before 1975 with high-energy demand. Among them one third is multi-owner, multi-story residential buildings. (“(WBCSD) World Business Council for Sustainable Development, Geneva” 2009). In the past few years, high-energy demand of existing buildings motivates retrofit campaigns and raises issues regarding building envelope performance (Masera et al. 2017a). Because heat loss through the building envelope is a key consideration. Some of the important measures used in the retrofitting process of the building envelope include external walls’ insulation, windows’ glazing type, air tightness (infiltration) and solar shading. While Santamouris and Dascalaki (Santamouris and Dascalaki 2002) suggest that the applying a thermal insulation layer is a common retrofit solution for old and historical building façades. However, a considerable fraction of existing building facades in Europe strongly articulated as historical meaningful facades and preserve appearance of heritage architecture is very serious. Moreover, the risk of interstitial condensation resulting from improper thermal retrofit can lead to



undesirable consequences, such frost damage, mould growth and unhealthy indoor environment (Ibrahim et al. 2014). In this regard, effective moisture control can reduce condensation risk and contribute to energy use reduction (F. Pacheco Torgal et al. 2016). Therefore, the best balance between reducing heat loss (thermal performance) and moisture control (hygro-thermal performance) is affected by characteristics and conditions of insulating system (e.g. locations of insulation layers, insulation thickness, etc.) (Ozel 2014).

In this context, a recently insulating plaster based on the (super)-insulating materials, silica aerogels with special properties (e.g. lightweight, ultra-low thermal conductivity, permeability and hydrophobicity behaviour), has been developed, which can be used in various building components and it is an effective option in case of buildings whose original façade appearance needs to be preserved specially to retrofit of building façade (Schuss et al. 2017). Baetens et al (Baetens Ruben, Petter Jelle Bjorn 2011) suggested aerogel as one of the most promising high performance thermal insulation materials for building applications. Thus, the main attention in this dissertation was drawn to use the simultaneously heat and moisture transfer models in building performance simulation to predict it's potential in reduction of condensation damage and energy consumption with regarding position in wall configuration and optimal thickness. Hopefully, using optimal thickness based on environmental assessments will support decision-making process, which leads to conservation of energy and environment with the best possible cost.

## **1.2 Background**

According to the Directive 2012/27/EU ([Http://www.buildup.eu/en](http://www.buildup.eu/en), n.d.), based on the conclusions lead by the Council on the Energy Efficiency Plan 2011, the construction sector causes 40% of the energy consumption. Building sector is responsible for one-third of global greenhouse gas emissions annually via consuming of heating and

cooling energy (Ürge-Vorsatz et al. 2015). In Europe, 9 billion square meters of the residential stock have been built before 1975 with high-energy demand. Among them one third is multi-owner, multi-story residential buildings. (“(WBCSD) World Business Council for Sustainable Development, Geneva” 2009). High-energy demand of existing buildings motivates retrofit campaigns and raises issues regarding building envelope performance. Often, the only acceptable solution for the energy efficiency improvement of the envelope is the internal retrofitting of the perimeter walls. The type of insulation selected for the retrofitting can affect the results, especially in case of inner retrofit. The use of novel and high performance insulation could be competitive to the conventional one, in terms of equivalent thickness for reaching the same performance. (Kosny, Fallahi, and Shukla 2013). Some of the important measures used in the retrofitting process of the building envelope include: external walls’ insulation, windows’ glazing type, air tightness (infiltration) and solar shading. In addition, multiple efforts are being undertaken to derive more efficient retrofit solutions. For example (El-Darwish and Gomaa 2017) showed that simple retrofit strategies such as solar shading, window glazing, air tightness then insulation can reduce energy consumption of an average of 33%. The result of another study (Santamouris and Dascalaki 2002) presented that the applying a thermal insulation layer is a common retrofit solution for old and historical building façades. Depending on the requirements to maintain the style and shape of the façades, this layer can be applied on the external or internal wall surface. They studied on 10 office buildings located in seven different climatic zones around Europe, by performing the energy audits and monitoring activities, specific experiments as well as an assessment of the potential of proposed retrofitting scenarios for each building.

Aerogels were discovered in the early 1930s by Kistler (Kistler 1930). Masera et al (Masera et al. 2017b) presented an innovative technical retrofit solution: a lightweight, aerogel-based wallpaper that can be

easily installed on the inner side of perimeter walls. The system is composed of an aerogel-impregnated textile layer, forming the insulating core, and a fabric finishing that can be easily installed and replaced thanks to a bespoke tensioning device. The cold bridges, thermal capacity and environmental impact of system were analyzed. Baetens et al (Baetens Ruben, Petter Jelle Bjorn 2011) suggested aerogel as one of the most promising high performance thermal insulation materials for building applications. Within this work, a review is given on the knowledge of aerogel insulation in general and for building applications in particular.

### **1.3 Research Objectives**

The main objective of this study was to investigate effect of aerogel plaster location (interior and exterior layer) and thickness on thermal and hygro- thermal performance of residential building to retrofit of building façade. This research has been conducted using two types of methods: computational and experimental. On the one hand, simulation software based on mathematical calculation of heat and moisture transport were used to the predicting hygric and thermal conditions in building envelopes as a computational method. On the other hand, experimental measurements were performed via application of silica aerogels on the external walls of a historical building façades as a case study. Long term-monitored data provided the basis calibration and generation more accurate initial simulation model.

### **1.4 Structure of the Work**

This dissertation is structured in terms of seven chapters. Chapter 2 studies the importance of building retrofit and how renovation measures can be effective in controlling the heat loss from building envelope, especially the significant number of residential buildings in need of renovation in Europe. Humidity control also plays an important role in this area. For this purpose, new material called Aerogel with simultaneous heat and moisture control with unique properties has

been introduced as super thermal insulation. Chapter 3 focuses on simultaneous heat and moisture transfer in buildings components and its assessment method. Chapter 4 deals with simulation model calibration as an initial effort toward enhancing the reliability of building performance simulations. The resulting calibrated simulation model also serves as a platform for evaluation of the characteristics and configuration of the insulating system in Chapter 5, whose output (e.g., locations of insulation layers, insulation thickness). Finally, Chapter 6 discusses the research conclusions and future outlook. In addition, Chapter 7 lists the references, figures and tables.

## CHAPTER 2.

### GENERAL APPROACH

#### 2.1 Building Retrofit

In accordance with the Energy Efficiency Directive (EED) in Europe, emission of CO<sub>2</sub> and greenhouse gases effect due to burning fossil fuels must sharply reduce. According to the World Bank collection of development indicators in the EU, 50% of final energy consumption in 2012 was allocated to heating and cooling which, 84% of heating and cooling is still produced from fossil fuels that buildings represent 40% of final energy consumption. Meanwhile, a large part of the existing building stock in Europe was built before 1919 and 70% of them are highly inefficient. With a view to improving energy performance of the building stock and achieving the Union objective of reducing greenhouse gas emissions by 80-95 % by 2050 compared to 1990, renovation is one of the essential foundations for significant energy demand reduction. Consequently, it will lead to reducing in energy costs for households and businesses and important environmental impacts (European Parliament 2012). The residential building stock accounts for about 70% of the total building stock, the non-residential stock, with its share of 30% is far from negligible. The basic data of energy balances for 2004 from the International Energy Agency (Itard et al. 2008) presents that the residential sector is responsible for 30% of the total final energy consumption, the non-residential sector for 11% and the construction industry for only 2%. Dwellings are generally divided into single-family houses and multi-family houses. In Austria, there is approximately the same number of multi-family dwellings and of single-family dwellings (around 50% for each). Retrofitting of existing buildings presents by far the largest potential for the incorporation of renewable energy technologies and energy efficiency measures into buildings (Santamouris and Dascalaki 2002). In terms of retrofitting of the existing building, heat loss through the building envelope is a key consideration

because the users for comfort have to be produced more energy. Therefore, more renovation of existing building façade has the potential to lead to significant energy savings potentially reducing the EU's total energy consumption and lowering CO<sub>2</sub> emissions (El-Darwish and Gomaa 2017). Some of the important measures used in the retrofitting process of the building envelope include: external walls' insulation, windows' glazing type, air tightness (infiltration) and solar shading. Meanwhile, the role of exterior walls in reducing heat losses as a large part of the building envelope should not be underestimated. It should not be underestimated that more than half of existing building in Europe strongly articulated as historical meaningful facades and preserve appearance of heritage architecture is very serious. Based on Federal Heritage Office regulates building renovation's statement in Austria, the main goal is maintenance of historical buildings with minimum altering of original facades. According to the Austrian Institute of Building Technology (OIB), application of exterior plaster insulation is acceptable only in the following cases:

- Comparable insulating effect cannot be obtained by other types of insulation
- Insulating materials are similar to those used in original structure
- Layer thickness, material properties of the original plastering are close to newly insulation, the connections, shapes and dimensions of the architectural elements of the façade must correspond to the historical architectural concept
- Original construction is protected from damage via these measures

## 2.2 Moisture control

On one hand, heritage buildings can only survive if properly maintained. Increasing the demand for higher thermal comfort lead to install the number of heating and air-conditioning systems in buildings. If the

building envelope has not been designed to handle the newly imposed temperature and vapour pressure gradients condensation may occur (H. M. Künzel and Holm 2009). The occurrence of moisture problems can lead to a host of undesirable consequences for construction and energy efficiency. They can be wood decay, mold growth, corrosion of metals, damage to materials and finishes from expansion or contraction, loss of strength in building materials to the point of structural failure, poor indoor air quality and loss of thermal resistance in wet insulation (Ibrahim et al. 2014). Therefore, appropriate moisture control is a prerequisite for energy efficient and damage free design of restoration and rehabilitation measures for existing buildings (H. M. Künzel and Holm 2009). On the other hand, good moisture control design depends on a variety of parameters such as climate conditions and construction type, which changes from region to region. Therefore, it is almost impossible to establish general rules that apply everywhere and for each construction. This is the reason why the considerable scientific effort was committed to the development of hygro- thermal models that help to predict the transient temperature and humidity conditions in building envelope components like walls and roofs.

### **2.3 Silica Aerogel**

In this context, regards to the retrofit of existing buildings with considering the thermal performance based on keeping the original historical facades and prevent of condensation risk and moisture damage, insulating materials with recently insulating plaster based on the (super)-insulating materials aerogels have growing interest (Schuss et al. 2017). Although it was discovered in the early 1930s by Kistler (Kistler 1930). The name "aerogel" refers to the way of its production: is technically a gel, with a gas or vacuum filling its pores instead of a liquid. Silica aerogel is the most widely used type of aerogel, which has the chemical formula  $\text{SiO}_2$ . It is insulating glassy material widely high-tech and building applications. The high potential of silica aerogels is due to their unusual solid material properties. Silica aerogel consist of a

cross-linked internal structure of  $\text{SiO}_2$  chain with a large number of air-filled pores. Due to its extraordinary small pore sizes and high porosity, the aerogel achieves its remarkable physical, thermal, optical and acoustical properties, while on the other hand this also results in a very low mechanical strength (Baetens Ruben, Petter Jelle Bjorn 2011). The high porosity makes aerogels the lightest solid material known at the moment, which is composed of 98% air. It can result in a bulk density as low as  $3 \text{ kg.m}^{-3}$ , e.g. compare with the density of air of approximately  $1.2 \text{ kg.m}^{-3}$  (F. Pacheco Torgal et al. 2016).

### 2.3.1 Structure characterization

Silica aerogel is characterized by 3-dimensional network of molecules, containing solid state and pore structure, filled with air or vacuum. This solid framework consists of nanoparticles of silica - the oxide of silicon. The way that these nanoparticles connect together network differs and mostly depends on a process of gel production. Primary nanoparticles of silica aerogel, sized 2-50 nm in its diameter are connected together into bigger spherical particles of a size 50 nm-2  $\mu\text{m}$  (2000 nm) in its diameter. As the next step, they are linked together and result as cross-linked polymers resembling a string of pearls. In case of acid-catalyzed gel production process, smaller nanoparticles do not connect together into bigger structures and thus form a structure resembling a leaf-like shape (["http://www.aerogel.org/"](http://www.aerogel.org/) 2019). Generally, synthesis of aerogel is divided into three main steps: gel preparation, aging of the gel and drying of gel under special conditions. They are dried by the method of supercritical drying, so that high porosity of a wet gel state is also kept in dried samples (Figure 1).



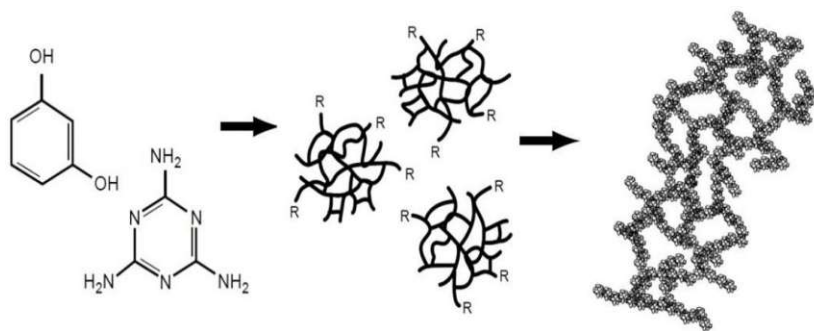


Figure 1: Structure of silica aerogel (Xian Yue, Junyong Chen, Huaxin Li, Zhou Xiao 2020)

### 2.3.2 Gel preparation

Firstly, the gel is prepared by using a sol-gel process, in which the solid components of the gel are spread in a dissolvent liquid and after some chemical reactions the mixture reaches the gel point. Typical precursors for silica aerogel production are tetramethylorthosilicate (TMOS), tetraethylorthosilicate (TEOS), polyethoxydisiloxane (PESD), methyltryethoxysilane (MTES), silicon alkoxide etc (Shukla, Fallahi, and Kosny 2012). Process of hydrolysis requires a catalyst, i.e. acid or base catalysis reaction. The sol changes its state to a gel, when distributed nanoparticles group together and form rigid SiO<sub>2</sub> network of particles after their collision. Silicon alkoxides are very specific materials of a high price and represent a challenge in a way of aerogel commercialization. This fact forces replacing silicon alkoxides with water glass or sodium silicate Na<sub>2</sub>SiO<sub>3</sub>, as they represent a cheaper raw material.

### 2.3.3 Aging of the gel

After a sol reaches the gel state, its aging process begins. It might be kept in a solvent for a sufficient amount of time till hydrolysis and condensation processes are finished. Meanwhile strengthening of a gel continues, its mechanical and permeability properties can be improved by controlling the water content and concentration of the solvent and its pH level. This process was researched by (Smitha et al 2016), who found that bulk density and shrinkage decreased, in addition to the

expansion of surface area, pore dimensions and its volume with the increase of TEOS concentration in a solvent. During the process of aging, two mechanisms take place, which affect properties and structure of aerogel: transport of the material to the neck region and dissolution of smaller particles into bigger ones (Soleimani Dorcheh and Abbasi 2008). Transport of material is not affected by the process of convection due to solid state of the gel, while diffusion itself is influenced by the thickness of gel. At the end, required time for each mechanism increases with aging of gel, which makes production of aerogels less practical.

#### *2.3.4 Drying of the gel*

Drying is the final stage in the production process of aerogel. In this step, the liquid inside the gel acquires a state of a gas and is removed from the gel network. Though, due to the surface tension of the liquid, it might damage the structure of gel network along with the process of evaporation. As a result, gel volumetric shrinkage and network collapse might happen. To avoid this scenario, the aged gel is placed under the supercritical conditions. These conditions facilitate the absence of surface tension; as distinct liquid-vapor phase boundary is absent. Supercritical conditions suppose low or high temperatures depending on a respective liquid (mainly alcohols, some water and catalyst), but high pressure is a necessary condition. As a result, big surface area of silica aerogel with high porosity and low density is produced.

#### *2.3.5 Thermal conductivity*

Aerogels have a very low thermal conductivity value about  $0.015 \text{ Wm}^{-1}\text{K}^{-1}$ . Baetens et al. (Baetens Ruben, Petter Jelle Bjorn 2011) suggested aerogel as one of the most promising high performance thermal insulation materials for building applications. When the Nanoporous material of aerogel is placed in moist environment, the solid backbone of the material will adsorb the water vapor from the air, and then the adsorbed water vapor will form a liquid water film attached to

the surface of the solid backbone. Since the thermal conductivity of water is much higher than air, the adsorbed water film will enhance heat transfer in the material and the thermal conductivity of aerogel increases up to  $0.020 \text{ Wm}^{-1}\text{K}^{-1}$ , however they are remaining in the superinsulation range (Nocentini, Achard, and Biwole 2018) .

### 2.3.6 *Acoustic properties*

Less studies are available on the acoustic properties of aerogels (T. W. L. Forest, V. Gibiat 1998) (A. H. L. Forest, V. Gibiat 2001) (P. Ricciardi, V. Gibiat, n.d.) (P. Ricciardi, n.d.) (Buratti, Merli, and Moretti 2017). In a first study in 1998 (T. W. L. Forest, V. Gibiat 1998) the acoustic propagation in aerogels was investigated and were compared with those of a glass wool sample. Small and large granule aerogels were considered and it was found that the glass wool exhibits better absorption properties than large granule aerogels, while small granules have a higher attenuation than glass wool. Furthermore, it was demonstrated that the best behaviour of aerogel granules as audible sound absorbers was found when used in coupled layers with different granule sizes. It is confirmed in (P. Ricciardi, V. Gibiat, n.d.), a maximum attenuation of about 60 dB was obtained for a sample constituted by three layers 2 cm thick of decreasing diameter (3 mm, 1 mm, and  $80 \mu\text{m}$ ). Granular aerogels with very low granule size (powders) were also used to simulate the snow behaviour, in order to use the acoustic emissions to predict avalanches (P. Ricciardi, n.d.).

### 2.3.7 *Safety and health aspects of aerogel*

Drying aqueous solutions of sodium silicate produce Silica aerogels. The very low dust density has prevented the widespread application of these materials in the past because of the potential health hazards, which would occur as a result of inhalation (Cuce et al. 2014). Aspen aerogels presented a report about the potential health problems, which may be caused by aerogels as shown in Table 1 (["https://www.aerogel.com/resources/health-and-safety/"](https://www.aerogel.com/resources/health-and-safety/) 2019).

Table 1: Potentials hazardous effect of aerogels on human health

Potential	
health effects	Explanation
Inhalation	Inhalation of airborne dusts may cause mechanical irritation of the upper respiratory tract
Eye contact	Exposure to dust from this product can produce a drying sensation and mechanical irritation of the eyes
Skin contact	Skin contact with dust from this product can produce a drying sensation and mechanical irritation of the skin and mucous membranes
Skin absorption	Material will not absorb through skin
Ingestion	This material is not intended to be ingested (eaten). If ingested in large quantity, the material may produce mechanical irritation and blockage.
Acute health hazards	Dust from this product is a physical irritant, and may cause temporary irritation or scratchiness of the throat and / or itching and redness of the eyes and skin
Chronic health hazards	In 2006, the International Agency for Research on Cancer (IARC) reclassified titanium dioxide as “possibly carcinogenic to humans” (Group 2B) based on animal experiments. In the draft Titanium Dioxide Monograph (Vol. 93), IARC concluded that the human carcinogenic studies “do not suggest an association between occupational exposures as it occurred in recent decades in Western Europe and North America and risk of cancer”
Medical conditions Aggravated by exposure	Excessive inhalation of dust may aggravate pre-existing chronic lung conditions including, but not limited to, bronchitis, emphysema, and asthma. Dermal contact may aggravate existing dermatitis

### 2.3.8 Building application of silica aerogel

Silica aerogels are an innovative alternative to traditional insulation especially whereas lack of insulation space, dynamic building physics and preserving historical features are a challenge. Due to their high thermal performance, flexible, hydrophobic and breathable format they are, more and more, entering the building sector in a wide range of applications including: Walls (internal & external), Floors, Ceilings, Dormers and Pitched Roofs, Terrace & Balcony, Gutter & Soffit Window, door and fenestration inserts, Point, repeating & linear thermal bridging treatment, Services, ducts, hot water pipework. In addition to those applications, aerogel is preferred for several purposes such as sound insulation, fire retardation and air purification. Although their cost still remain high compared to the conventional insulating materials. However, intensive efforts are going on to reduce their manufacturing cost and develop novel types of aerogels.

Aerogel applications in buildings for day lighting goals become widespread. Two examples of translucent aerogel insulation as a high performance thermal insulation solution for day lighting purposes are illustrated in (Figure 2 to Figure 5) (Berardi 2015). Another application is opaque ones or granular aerogel-based translucent insulation materials, which used for thermal protection of envelopes, including walls and roofs. (Figure 6) (Baetens Ruben, Petter Jelle Bjorn 2011). Wong et al. suggested that transparent insulation materials not only performed similar functions to opaque insulation, reducing heat losses and controlling indoor temperatures but also allowed solar transmittance of more than 50%. With a thickness of less than 20 cm, it could provide a financial return to building occupants (Wong, Eames, and Perera 2007).



Figure 2: Examples of translucent Silica aerogel insulation block form (Berardi 2015)



Figure 3: Sample of the monolithic aerogel panel used in the glazing units (Berardi 2015)

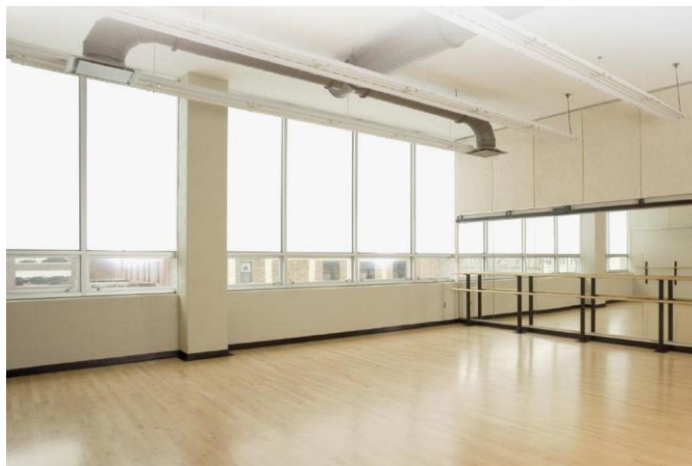


Figure 4: Granular filled aerogel windows: Detroit School of Arts, MI, USA (Berardi 2015)



Figure 5: Granular filled aerogel windows: Nobel Halls at SUNY Stony Brook, NY, USA applied over large areas in new buildings for day lighting purposes (Berardi 2015)



Figure 6: Rendering Fixit 222 with aerogel (Proskurnina, n.d.)

Because of combination of a low thermal conductivity and a high transmittance of daylight and solar energy, Aerogel is considered one of the interesting translucent and transparent insulation materials. Aerogel glazing provides diffuse natural light and good thermal comfort, due to the low U-value the inside temperature of the aerogel glazing is near the inside air temperature. Figure 7 shows the developed a granular aerogel based window in Germany by ZAE Bayern, which is stacked in a 16mm wide poly methyl methacrylate (PMMA) double skin-sheet, between two gaps (i.e. of either 12 or 16mm in width and

respectively filled with krypton or argon) and glass panes (Beck et al. 2002).

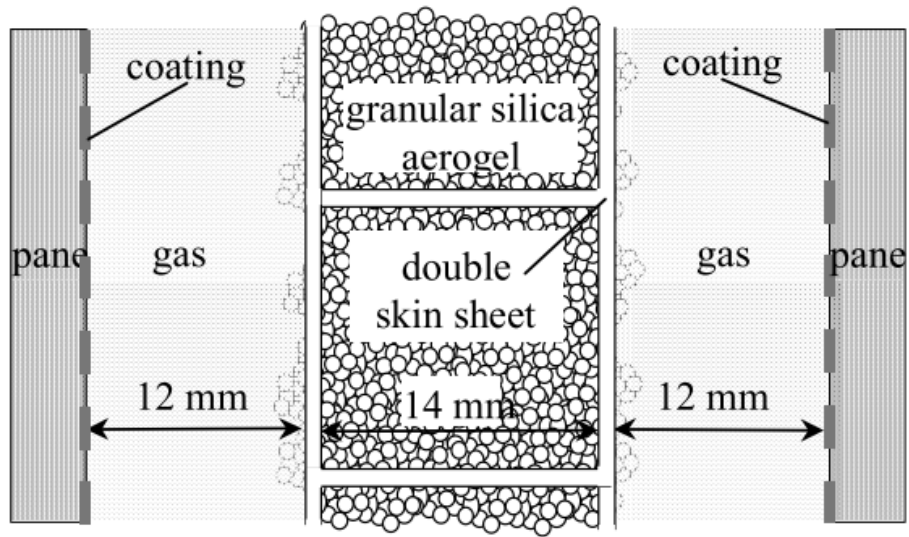


Figure 7: Cross-section through the granular aerogel based glazing, consisting of two glass panels with a low-e coating on the inside, two gaps and an aerogel-filled PMMA double-skin-sheet double-skin-sheet (M. Reim, W. Körner, J. Manara, S. Korder, M. Arduini-Schuster, H.-P. Ebert 2005)



# CHAPTER 3.

## SIMULTANEOUS HEAT AND MOISTURE TRANSPORT IN BUILDING COMPONENTS

### 3.1 Introduction

Recently, there is an increasing demand for calculative methods to assess the moisture behaviour of building components. Because the water leads not only structural damage but also the high initial moisture content has strong impact on indoor condition and energy consumption. Especially in cold climate where the moisture freezing in building envelope would occur in winter. The amount of moisture diffuse from or into the building envelope interior surface affects the indoor humidity level and latent heat load of building heating or cooling energy calculation, which are quite often ignored in whole building energy analysis tools. While the heat and moisture transfer and moisture phase change at inner building envelope affect the heat transfer coefficient and therefore heat transferring rate, which are important parameters for a building whether energy-saving or not. So, it is important to accurately predict the hygro-thermal states of building envelope to achieve useful envelope parameters result and take them (durability, indoor humidity level and energy performance of the building) into account as part of an optimized building design simultaneously (Kong and Wang 2011). In the last century, the physics of heat and mass transfer in porous media has been largely studied and a review of the most widely used methods is presented. A brief overview of the methods proposed by various authors for taking into account the effect of a fluid flow over the heat and mass transfer in a porous media is presented at the end of the chapters. In this chapter, a brief explanation of the physical mechanisms of heat and moisture transfer in porous materials and air is exposed.

### 3.2 Hygric effect on heat storage and transport

The principles of calculating the thermal behaviour of building components in dry condition are known in building physics. Since this study is concerned primarily with moisture transport and its effect on heat transport, we will not deal with the pure temperature dependence of thermal quantities such as heat capacity, thermal conduction, specific heat of melting and evaporation. The hygric effects on these quantities are however so important that they have to be dealt with (H. M. Künzle 1995).

#### 3.2.1 Heat storage in moist building materials

The heat content of a material under isobaric conditions is called the enthalpy. In the temperature range, which is of concern in building physics, there is an approximately linear relationship between the enthalpy of a material and its temperature. The enthalpy of a dry building material, related to the enthalpy at 0 °C, is therefore described by means of the following equation:

$$H_s = \rho_s c_s \vartheta \quad \text{Eq. 1}$$

where

$H_s$	[J/m <sup>3</sup> ]	enthalpy of the dry building material
$\rho_s$	[kg/m <sup>3</sup> ]	bulk density of the building material
$c_s$	[J/kgK]	specific heat capacity of the building material
$\vartheta$	[°C]	temperature

In the case of moist building materials, we must add to this enthalpy the enthalpy of the water contained in the material. However, the enthalpy of the water depends on the existing physical states.

### 3.2.2 Thermal conduction in moist building materials

This term is used "thermal conduction in moist building materials" only to describe the effect of localized water on heat transport. While the evaporation and condensation of transported moisture also contributes to heat transport, it cannot be described in practical terms by means of the thermal conduction equation. Information about the dependence of thermal conductivity on the water content can be found in (Cammerer, J. und Achtziger 1985) for various building materials. Since standard measurements also include the effect of water vapour diffusion, the results of measurements in the guarded hot plate apparatus for diffusible materials, such as mineral wool, can only be used with caution. According to (H. Künzel 1986), the following relation can be used to calculate the moisture-dependent thermal conductivity  $\lambda(w)$  of mineral building materials:

$$\lambda(w) = \lambda_0(1+b \cdot w/\rho_s) \quad \text{Eq. 2}$$

where

$\lambda(w)$	[W/mK]	thermal conductivity of moist building material
$\lambda_0$	[W/mK]	thermal conductivity of dry building material
$\rho_s$	[kg/m <sup>3</sup> ]	bulk density of dry building material
$b$	[%/M.-%]	thermal conductivity supplement

Supplement  $b$  indicates by how many percent the thermal conductivity increases per mass percent of moisture. Its value is determined by the type of building material, but in the case of hygroscopic materials, it is largely independent of their bulk density.

### 3.3 Heat and moisture transfer at building component boundaries

The heat and moisture exchange between a building component and its surroundings can be described by means of boundary conditions of the first, second and third kind. Boundary conditions of the first kind, where

surface conditions are the same as the ambient conditions, occur in terms of heat and vapour transport only when the building component is in contact with water or the earth. In the case of liquid transport, this boundary condition applies when the component surface is completely wetted from rain or ground water. Boundary conditions of the second kind, which require on the surface a constant heat or mass flow, characterize the influence of solar radiation on heat transport and the uptake of rain water when the surface is not completely wetted. Symmetry conditions and adiabatic or water and vapour-tight conditions are covered by zero flows at the component boundaries. Boundary conditions of the third kind, which require a transitional resistance between the component surface and its surroundings, constitute the most frequent kind of heat and moisture exchange. When two different kinds of boundary conditions occur simultaneously, as in case of solar radiation and convection at building facades, this can be covered in the solution by using appropriate source terms (H. M. Künzle 1995).

### **3.4 Assessment of the calculation method**

Below, it will be summarize the new calculation techniques and functional characteristics of the newly developed calculation method, which in some respects clearly differs from previous models. Subsequently, it will be assess the Methodologies – new calculation vs. previous models.

#### *3.4.1 New calculation techniques and functional characteristics*

A comprehensive list of studies and calculation methods to quantify the moisture transport in building materials was already compiled by Kießl and Gertis (Kießl 1983), (Kießl, K. und Gertis 1980). In spite of the theoretical possibility of converting one potential into another, the choice of these potentials is of great importance for the general applicability and accuracy of mathematical models and the computer programs developed from them. Since in porous materials moisture can

move in vaporous or liquid form, with different driving forces, most publications assume two or more potentials for moisture transport.

Calculation methods are still being developed today, which as the standard method based on Glaser (Glaser 1985) in standard DIN 4108 (4108, n.d.) - consider only the vapour transport in building components. These methods use simplified calculation techniques to determine moisture storage through sorption and moisture dependence of vapour diffusion resistance. One of the first to study thoroughly the moisture movements in porous materials under the influence of temperature gradients was Krischer (Krischer, O. und Kast, n.d.). By analyzing the water content of sand wetted and dried in temperature gradients, he discovered that there are two transport mechanisms for material moisture, which may also act against each other. One is vapour diffusion, which at room air temperature can be described. Krischer called the other transport mechanism "capillary water movement", and he attributed it to the capillary suction stress, which develops as the result of curved water surfaces in the pore system of moist building materials. For capillary-active building materials with a broad pore size spectrum he derived a material-specific connection between water content and capillary pressure, so that the moisture transport in the liquid region, it can be described with the water content as the driving potential.

The method has been introduced was developed for the calculation of the simultaneous one and two-dimensional transient heat and moisture transport in multi-layered building components. The method takes into account regarding the hygric material properties of porous building materials. This means that as far as mineral building materials are concerned, we assume that the vapour diffusion resistance is not moisture- dependent, and that the transport phenomena observed in higher moisture regions, which increase vapour diffusion under isothermal conditions, are allocated to liquid transport.

### 3.4.2 *Hygro-thermal assessment*

An alternative standard is increasingly being recognized as the way forward. BS EN 15026:2007 'Hygro-thermal performance of building components and building elements. Assessment of moisture transfer by numerical simulation.' Hygro-thermal assessment is based upon the analysis of heat; vapour and moisture transfer through the elements of a building. The data provided by this method of assessment provides an accurate measure to the temperature, relative humidity and water content within the elements of a building measured over a specified time period. The use of hygro-thermal assessment employs sophisticated computer modelling to simulate the interactions between building envelopes, building services and the use of buildings. Hygro-thermal analysis will consider different climatic conditions and realistically evaluate the potential moisture levels in building components, identifying weaknesses, and thus enabling these to be corrected at the design stage (Challenge 2018).

### 3.4.3 *Accuracy of risk assessment methods*

There is a growing understanding of the importance of condensation control for all areas of the building envelope, in order to control moisture, and protect both the building fabric and the health of its occupants. Previously the methods for the assessment of the likelihood of condensation have been limited and at best offered a simplified average with limitations, however the newly developed computer program called WUFI or WUFIZ [Wärme- und Feuchtetransport instationär zweidimensional = transient one or two-dimensional heat and moisture transport], provides the coupled equation system and the numerical solution technique. In order to provide more clarity in the methods of assessment available and their uses, it has been outlined a summary between the traditional Glaser method and the latest software using the WUFI method of calculation below.

#### 3.4.4 *The Glaser method*

Traditional methods of assessment have in the past been based on the Glaser method – a standard static interstitial moisture calculation. More designers are recognizing the limitations of this method, which offers a simplified approach, developed back in 1958 for use in lightweight buildings. The simplified calculation used by the Glaser method is based on average monthly temperatures, vapour pressure and steady state conduction of heat to determine if critical condensation points are reached within one year. The Glaser method identifies vapour diffusion, how easily water vapour can pass through the fabric of the building. However, limitations of this approach are that Glaser assumes vapour moves only one way (inside to outside). It completely omits the key feature of driving rain from its calculations, does not measure absorption or porosity, and therefore misses the potential risk attributed to the aspect of moisture storage (Challenge 2018). As it is well known, the method has a lot of limitations. It cannot handle heat and moisture capacity; neither can it handle air transfer through structures and capillary liquid flow. As a result, constructions that are qualified as good moisture design, may in reality, due to built-in moisture, precipitation and air exfiltration face the problems mentioned (Hagentoft et al. 2004).

#### 3.4.5 *The WUFI calculation method*

The A. Proctor Group advises its customers using WUFI® software, which is fully compatible with BS EN 15026, and dynamically predicts moisture movement and storage as well as condensation for each location. Using WUFI® enables architects, designers and developers to identify the likelihood and risks of condensation, and enables designs to be optimized for longevity of the building fabric, and for the health and wellbeing of the buildings occupants. WUFI® software was developed by the Fraunhofer Institute for Building Physics in Germany and provides detailed heat and moisture calculations based on local climate

conditions for building materials, multilayer components and even whole buildings. The designer is able to achieve a minute-by-minute prediction over a given period of years, as specified by the designer. The program considers a worst-case scenario with the injection of a moisture source at the source to predict the robust drying out of the fabric build up. A further enhancement of using the WUFI® software is that external weather including driving rain and solar radiation is predicted in a cycle and the designer can choose the specific internal environment that the building will be exposed to. This has proven invaluable when assessing the correct position for high performance vapour control and vapour permeable membranes to ensure a healthy building fabric, whether it be roofs or walls (Challenge 2018).



## CHAPTER 4.

### HEAT AND MOISTURE MODEL CALIBRATION

#### 4.1 Introduction

Nowadays, whole building simulation is increasingly used in design of building heating, ventilation and cooling (HVAC) system. Presently difference between simulated and monitored building energy consumption has become a common research issue. In order to have accurate results and make simulation predictions match closely real consumptions, calibration has become an essential process to be carried out for building simulation. The two primary reasons for adopting this approach is that it allows (1) more reliable identification of energy savings and demand-reduction measures (involving equipment, operation, and/or control changes) in an existing building and (2) increased confidence in the monitoring and verification process once these measures are implemented. The present contribution includes a case study regarding the reliability of a hygro-thermal simulation tool as applied to an existing wall construction. Measured data was used to define the model's initial conditions and to evaluate the validity of the simulation results. Efforts were made to study the impact of input assumptions pertaining to boundary conditions and component's geometry representation (one versus two-dimensional) on the simulation accuracy.

#### 4.2 Methodology

Two types of criteria were considered in the framework of this retrofitted project by applying aerogel plaster:

- Building energy (heating and cooling) demand as a function of insulation thickness
- Moisture transfer and condensation risk as a function of the position of the insulation layer

### 4.3 Case Study Building

The case study of the present contribution is an office area in a historical university building of TU Wien, Vienna, Austria. The test areas were performed on three wall surfaces with different geographic orientation, south, west and north. Every facade is divided in smaller fields on which different finish layers have been applied, which can be seen in Figure 8.



Figure 8: View of the test areas on the south façade (fields 1-4), west façade (fields 5-8), and north façade (fields 9-10) (Schuss et al. 2017)

The old wall construction of the case study (with three layers including gypsum plaster, hollow brick masonry and lime cement plaster) was retrofitted by applying plaster system encompassing a highly-insulated aerogel layer (Fixit 222) (Fixit 2018) on the existing construction (Figure 9). When the plaster is fully dried out a mineral based undercoat stabilizer (FIXIT 493) is sprayed on the aerogel plaster to harden the surface and give it a better grip for the finishing layers. In the next step the fields got an additional reinforcement fabric mesh in an embedding mortar to prevent cracks and get a more stress resistant surface. To test different material variants, not all fields were done with this mesh. Than every field got its unique finishing layer which consists out of a grained material and silicate paint Röfix PE. Very important is that all this layers should be diffusion open due to the properties of the aerogel plaster. Table 2 shows the basic and hygro-thermal properties of the old wall construction and new aerogel plaster. Moreover, four combination of exterior plaster on fields 1 to 4 was detailed in Figure 10 and Table 3.

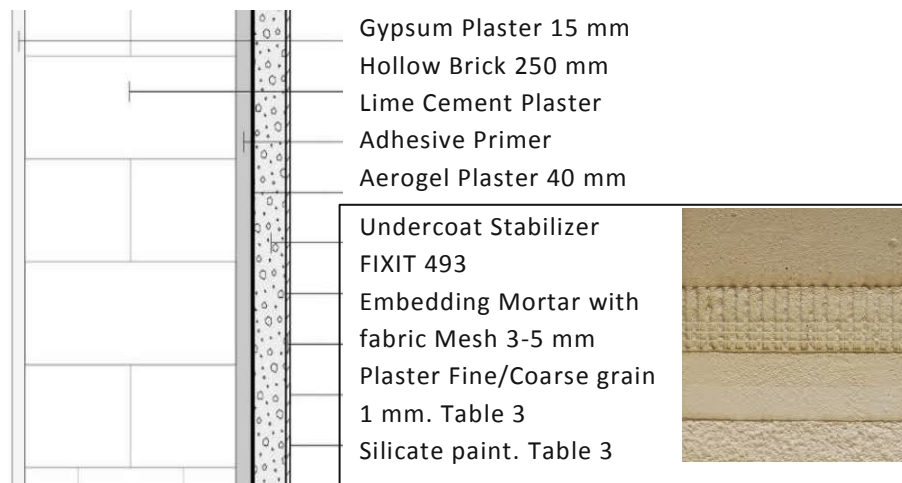


Figure 9: The layer section of tested facade

Table 2: Input data pertain to the thermal and hygro-thermal properties of material

	Properties	Unit	Röfix 380	Aerogel	Brick	Interior plaster
Basic	Layer thickness	[m]	0.002	0.04	0.25	0.02
	Bulk density	[kg·m <sup>-3</sup> ]	1000	220	1560	1721
	Porosity	[%]	0.24	0.92	0.38	0.31
	Specific heat capacity	[J·kg <sup>-1</sup> ·K <sup>-1</sup> ]	1000	1000	850	850
	Thermal conductivity (dry material at 10°C)	[W·m <sup>-1</sup> ·K <sup>-1</sup> ]	0.47	0.029	0.4	0.2
	Water vapor diffusion resistance factor	[-]	12	4	14.93	13
	Reference water content (RH 80%)	[kg·m <sup>-3</sup> ]	45	6.6	11.80	1.77
	Free water saturation (RH 100%)	[kg·m <sup>-3</sup> ]	210	213	368.9	264.2
	Water absorption coefficient (A-value)	[kg·m <sup>-2</sup> ·s <sup>-0.5</sup> ]	0.02	0.0004	0.51	0.30
	Moisture-dependent thermal conductivity supplement	[%·M <sup>-1</sup> ·% <sup>-1</sup> ]	8	0.5	8.51	3.23
Hygro-thermal						

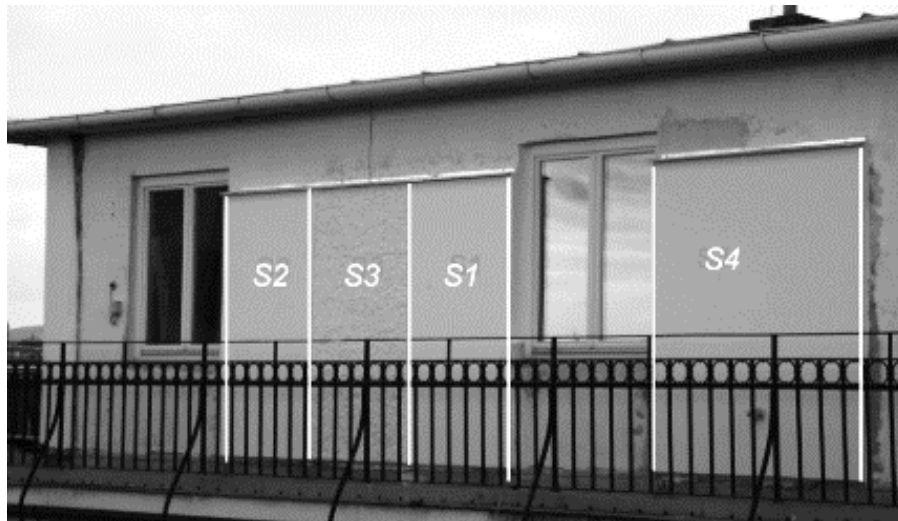


Figure 10: The south tested surface, which has divided four fields (Schuss et al. 2017)

Table 3: Combinations of exterior plaster of fields 1 to 4

Field	Plaster	Silicate paint	Sd-Value (m)	$\mu$ Value	Remarks
S2	Röfix 380 fine grained	Röfix PE 819 Sesco, lime wash	0.0002	12-15	Diffusion open, stores moisture
S3	Röfix 750 coarse grained	Röfix PE 225 Reno, silicate paint	0.01	20	Diffusion open
S1	Röfix 380 fine grained	Röfix PE 819 Sesco, lime wash	0.0002	12-15	Diffusion open, stores moisture
S4	Röfix 380 fine grained	Röfix PE 419 Etics, silicon resin paint	0.1	12-15	Diffusion open, water repellent

Figure 11 and Figure 12 show the application and smoothing of the aerosol plaster on the west façade on 28.04.2016. The subsequent production of the cover plaster system can be seen in Figure 13 and Figure 14.



Figure 11: Adhesive primer (on the left), application of FIXIT 222 with a plastering machine (on the right) (Proskurnina, n.d.)



Figure 12: Levelling off FIXIT 222(left), surface of FIXIT 222(right) (Proskurnina, n.d.)



Figure 13: Reinforcement mesh for corners of opening (left), application of reinforcement mesh (right) (Proskurnina, n.d.)



Figure 14: Applied reinforcement mesh (left), FIXIT 222 insulation plaster (right) (Proskurnina, n.d.)

#### 4.3.1 Monitoring data

In contrast to the other two walls, the south side was additionally equipped with sensors. A set of sensors have been installed by the Swiss Federal Laboratories for Materials Science and Technology (EMPA) within different layers of the south oriented construction, which enabled the in-situ measurement of temperature and relative humidity levels in different positions in the testing fields. Additionally, one sensor installed in the external layer of each field to measure the heat flow. Both of the position 0 and 1 lay directly under the exterior finishing layer, which position 0 is equipped with the heat flow sensor and position 1-5 are belong to temperature and relative humidity sensors. Position 2 and 3 are located on the surface before the aerogel plaster layer, from which number 3 is just a reserve sensor for in the case that the other one has any malfunction. Position 4 is directly in the middle of the masonry wall and the sensor in position 5 is directly applied on the interior surface of the existing plaster. Figure 15 shows the detailed section of the wall construction including the positions of the sensors.

In this study, utilized the monitored data of sensors in node 1, 2, 4 and 5 for all fields.

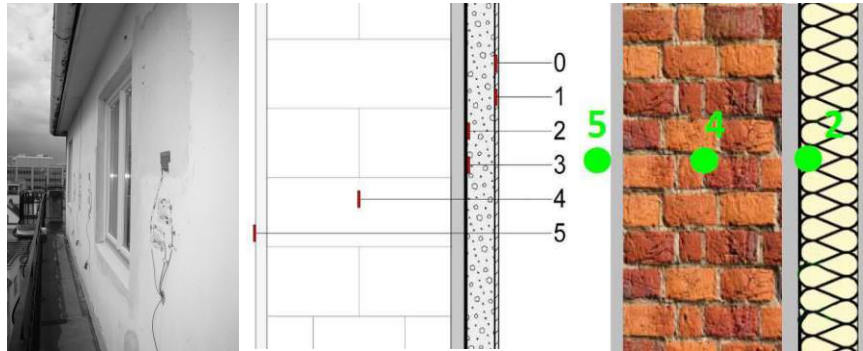


Figure 15: View of sensors before the application of the aerosol plaster and the Position of sensors in the layers of construction in south orientation (Schuss et al. 2017)

To determine the boundary conditions, additional sensors for temperature and humidity were installed. The interior sensor was hanged in the middle of the ceiling, directly behind the south facade and outside sensor was located on the south-facing test area, under the roof overhang. The solar radiation on the surfaces was additionally measured with a pyrometer directly next to the test areas (Schuss et al. 2017) (Figure 16).



Figure 16: The solar radiation and temperature / humidity sensors (Schuss et al. 2017)



The project was carried out over period of almost three years, which was beginning on 25.10.2013 at 01:00am and it last until 23.03.2016 1:00am. During the project, some problems with the sensors appeared but all of them were solved as fast as possible. Due to these problems, there were some days without data recording, which the Table 4 specifies the missed hours and days. In order to have an accurate calibration, this study utilized the monitored data for a period of one whole year of 2015 because it has fewer gaps in compared with other years.

Table 4: The period of missed measured data

<b>Date and time of missed measured data</b>	<b>Period</b>
12.12.2013 / 11:00 – 12:00	2h
01.01.2014 / 05:00 – 11:00	7h
02.11.2014 / 23:00 – 02.12.2014 / 08:00	10h
04.18.2014 / 20:00 – 04.19.2014 / 01:00	6h
05.06.2014 / 15:00 – 05.21.2014 / 10:00	455h – 19 days
05.26.2014 / 01:00 – 06.02.2014 / 10:00	189h – 8 days
09.09.2014 / 16:00	1h
09.29.2014 / 15:00 – 19:00	5h
10.10.2015 / 20:00 – 10.12.2015 / 07:00	33h

#### 4.3.2 Long-term evaluation of aerogel plaster with various finishings

The thermal insulation properties of the Aerogel high-performance plaster were examined in real operation based on the measured data from two heating periods. Specifically, the measured values for the heat flow and the surface temperatures inside and outside were used to calculate the (in situ) heat transfer coefficient according to the averaging method according to ISO 9869 (ISO 9869 1994). Figure 17 to Figure 19 show the heat flows measured in position 2 (between the existing wall and Aerogel plaster) for the heating periods 2013/2014, 2014/2015 and 2015/2016.

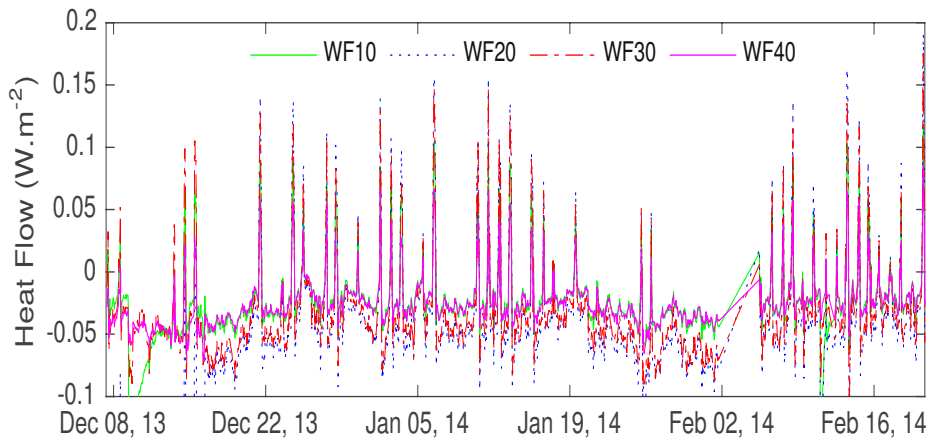


Figure 17: Heat Flow-Winter period 2013/2014

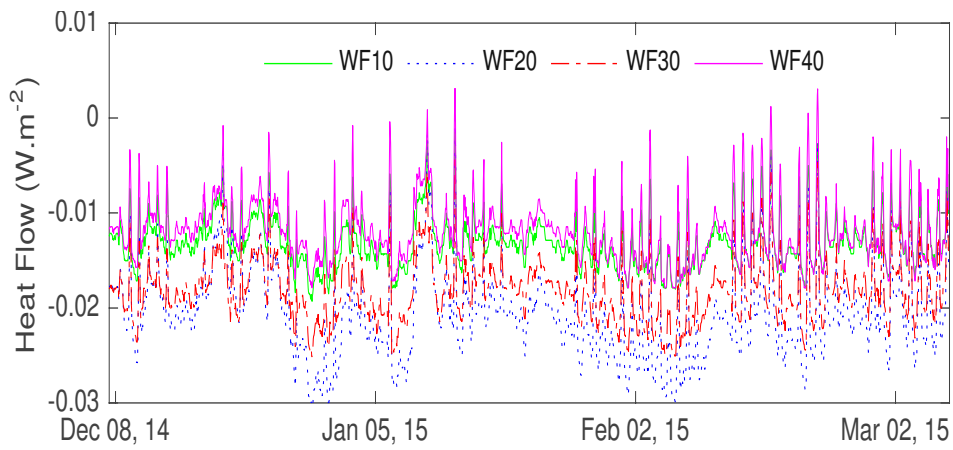


Figure 18: Heat Flow-Winter period 2014/2015

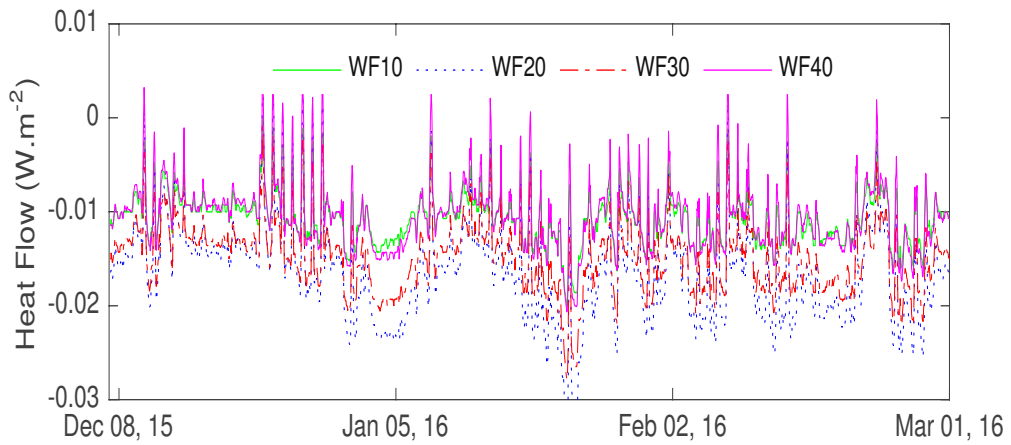


Figure 19: Heat Flow-Winter period 2015/2016

The south-facing test areas S1 to S4 have been metrological recorded since October 2013 to March 2016. Due to some missed data (Table 4), the analysis of the performance and the hygro-thermal behaviour was carried out based on whole period of year 2015 and the heating periods from the 1st of October to the 1st of March of year 2015. By the Box-plot diagram has been analyzed the distribution of data measurement (Temperature and Relative humidity).

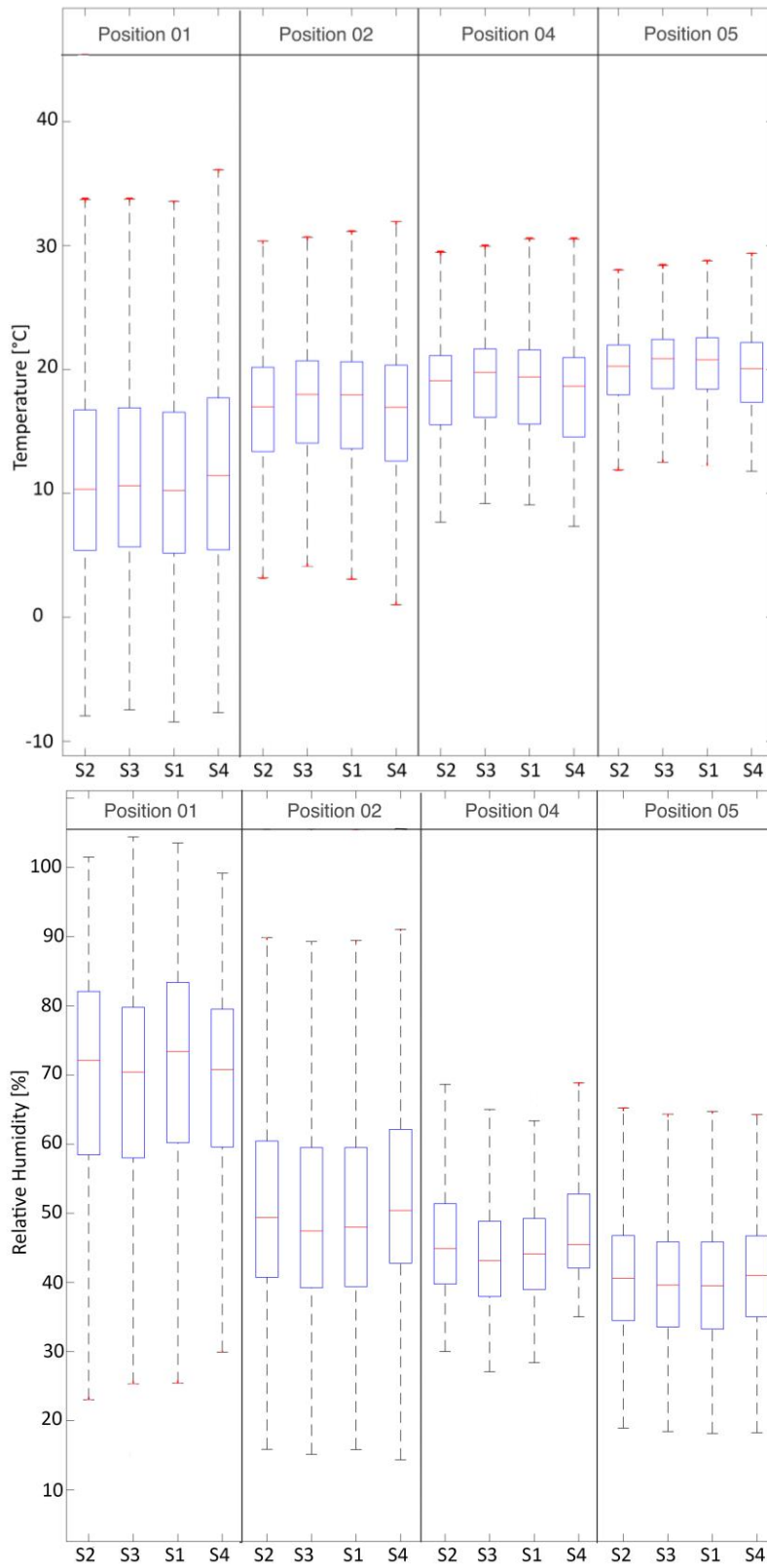


Figure 20: Distribution measured temperature and relative humidity in all positions of test areas / year 2015

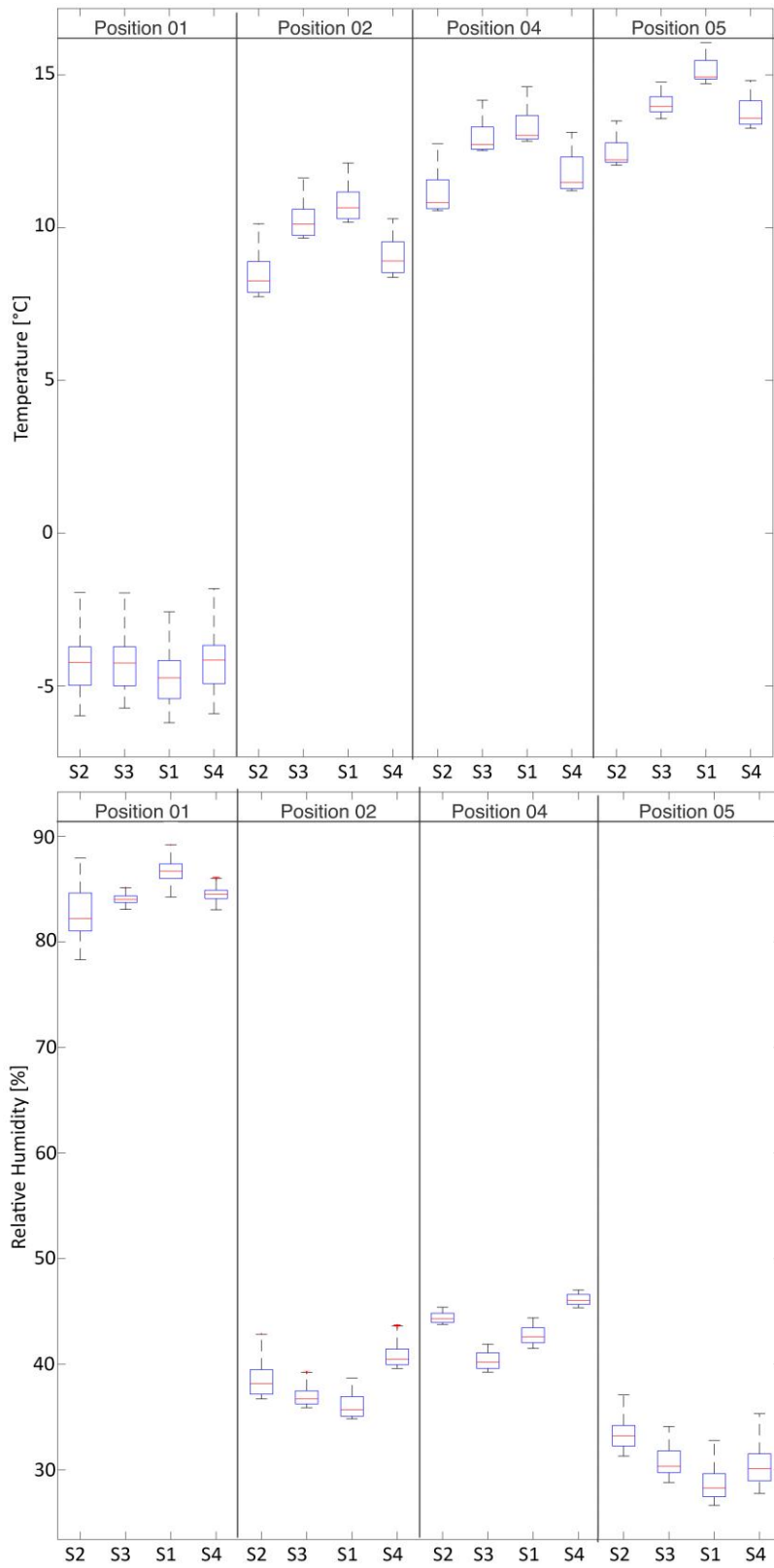


Figure 21: Distribution measured temperature and relative humidity in all positions of test areas / heating period 2015

Temperature profile shows no major differences between the fields. For a closer supervision of this topic the f value of the temperatures was calculated. This was performed by using the formula seen in equation 3, after the results were split in cold days ( $\theta_e < 0^\circ\text{C}$ ) and warm days ( $\theta_e > 24^\circ\text{C}$ ), accordingly to the outside temperature. This step has been performed for every sensor position in every field and presented in boxplot diagrams.

$$F \text{ Value} = \frac{\theta_{x,y} - \theta_e}{\theta_i - \theta_e} \quad \text{Eq. 3}$$

$\theta_{x,y}$ = Temperature of field x and position y

$\theta_e$ = Outdoor Temperature

$\theta_i$ = Indoor Temperature

For exactly investigation of humidity effect and reduction of condensation risk is needed to know the direct amount of water in the air, in other words calculation of specific humidity can be helpful in this study. The convert of relative humidity to specific humidity was performed with formulas in equation 4 -6

$$\omega = \frac{0.622 \varphi \cdot P_g}{P_a} \quad \text{Eq. 4}$$

$$\text{with } P_a = P - P_v \text{ and } P_v = \varphi \cdot P_g \quad \text{Eq. 5}$$

$$P_g = 611.2 \times \exp\left(\frac{17.62 \times t}{243.12 + t}\right) \quad \text{Eq. 6}$$

$P_g$ = Saturation vapor pressure [Pa]

$P_v$ = Partial Pressure water vapor [Pa]

$P_a$ =Pressure of dry air [Pa]

$P$ = Atmospheric Pressure [Pa] = 101325 Pa

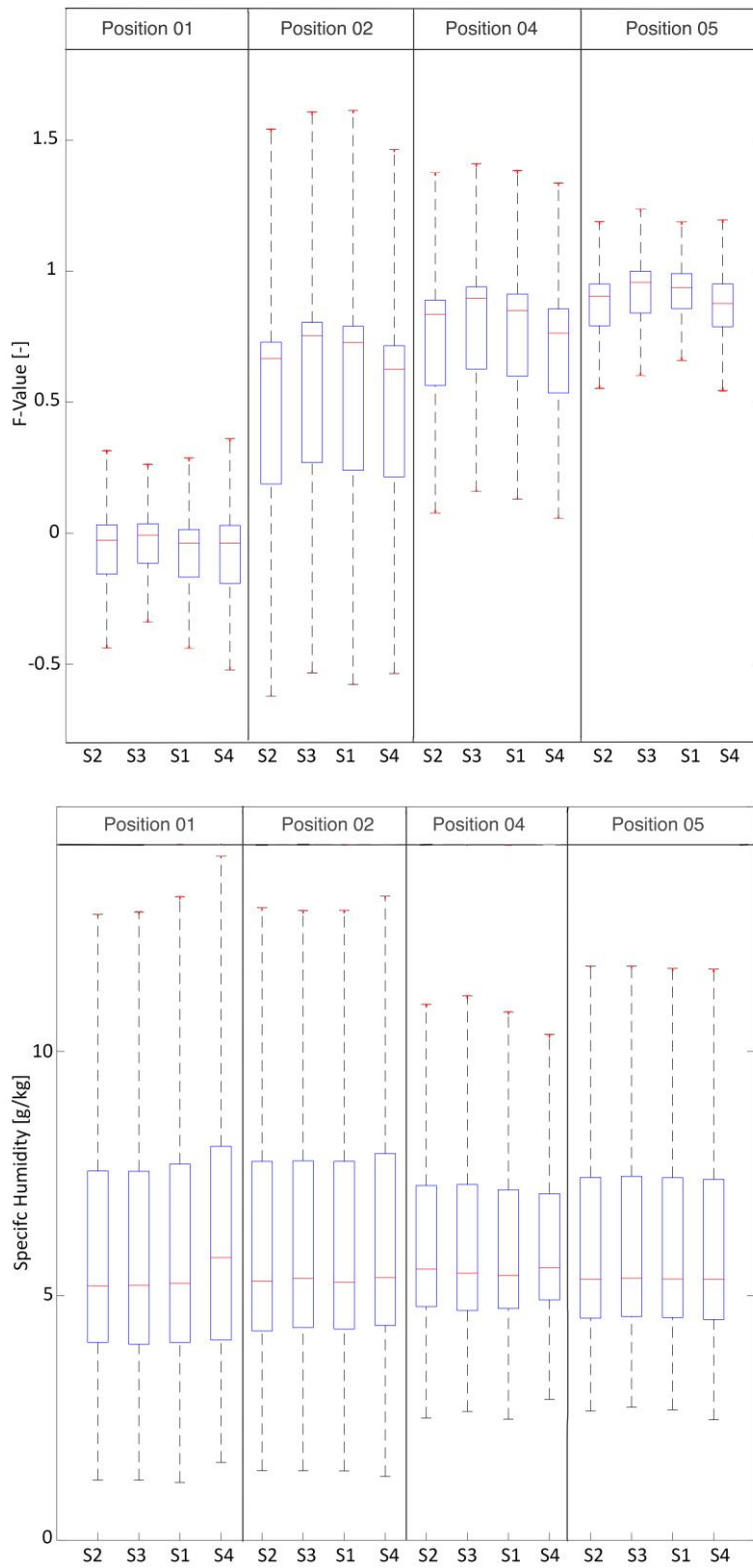


Figure 22: Distribution calculated F-value and specific humidity in all positions of test areas / year 2015

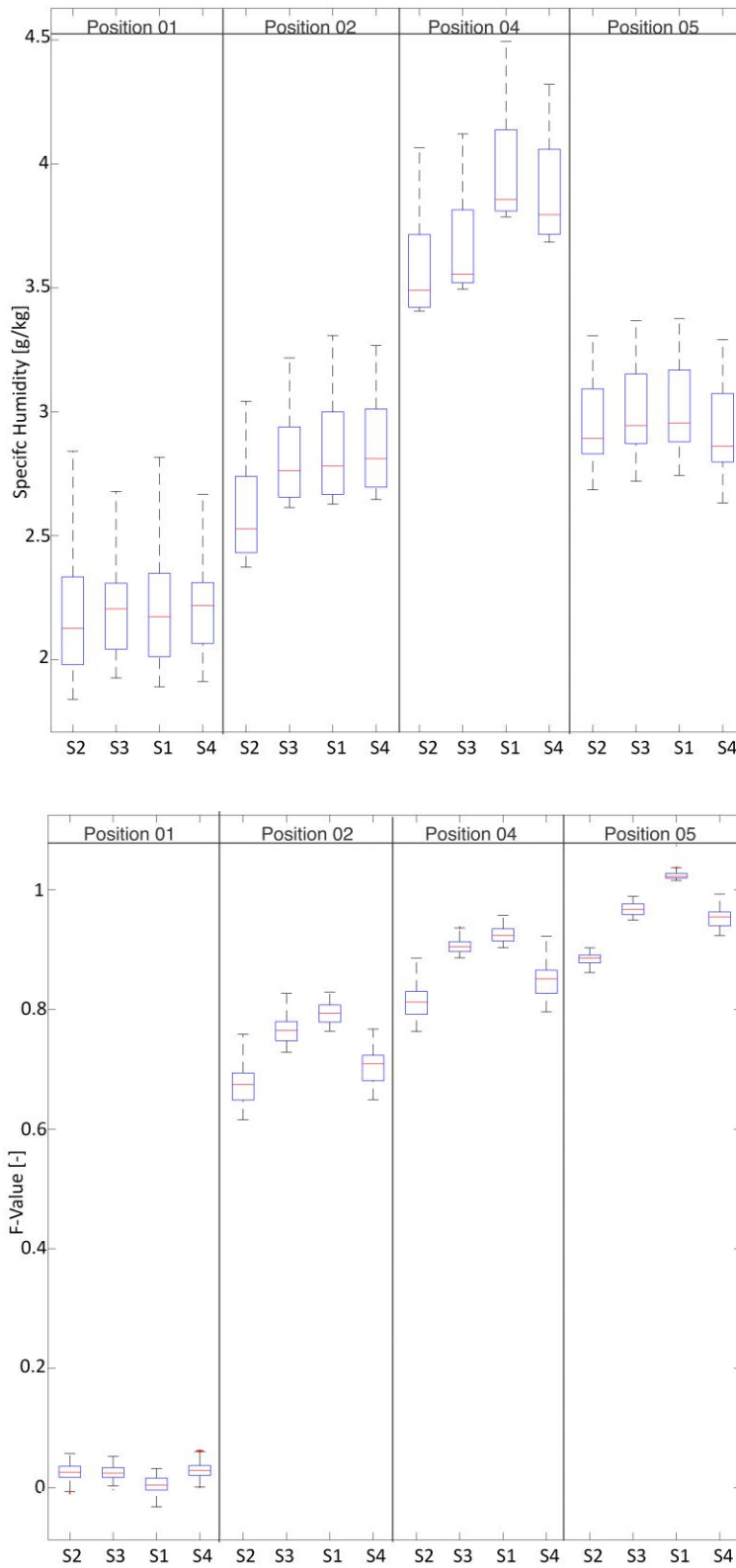


Figure 23: Distribution calculated F-value and specific humidity in all positions of test areas / heating period 2015



### 4.3.3 *Hygro thermal simulation with WUFI Pro and WUF 2D*

WUFI® is a family of software products that allows realistic calculation of the transient coupled one- and two-dimensional heat and moisture transport in walls and other multi-layer building components exposed to natural weather. WUFI® is an acronym for **W**ärme **U**nd **F**euchte **I**nstationär—which, translated, means heat and moisture transiency. WUFI® software uses the latest findings regarding vapor diffusion and moisture transport in building materials. The software has been validated by detailed comparison with measurements obtained in the laboratory and on IBP's outdoor testing field (WUFI 2011). Using WUFI® enables architects, designers and developers to identify the probability and risks of condensation, and enables designs to be optimised for long life of the building fabric and for the health and well-being of the building's occupants. WUFI® software was developed by the Fraunhofer Institute for Building Physics in Germany and provides detailed heat and moisture calculations based on local climate conditions for building materials, multilayer components and even whole buildings.

WUFI® Pro is the standard program for evaluating moisture conditions in building envelopes. Of all the programs in the WUFI Software Family, it is the easiest to use. WUFI® Pro performs one-dimensional hygro-thermal calculations on building component cross-sections, taking into account (where appropriate) built-in moisture, driving rain, solar radiation, long-wave radiation, capillary transport, and summer condensation. Other programs and traditional methods, like the Glaser-Method, do not consider these effects and are thus limited to only evaluating winter condensation effects. WUFI® Pro determines the hygro-thermal performance of building components under real climate conditions. This type of comprehensive dynamic hygro-thermal analysis is needed for accurate design and is required, for example, by the DIN EN 15026 standard. WUFI® 2D expands the scope of WUFI® Pro to two-dimensional analysis. A one-dimensional WUFI® Pro analysis cannot be

used when regions next to the line of interest have different heat and moisture responses. In particular, two-dimensional analyses are necessary for complicated geometries, such as building corners, window locations, and foundation connections and when there are non-uniform sources/sinks of heat and moisture. Compared to WUFI® Pro, the inputs for WUFI® 2D are considerably more complex, and the computational time is also significantly increasing. Given the ease-of-use of WUFI® Pro, it is most desirable to keep the analysis one-dimensional. Indeed, many situations, including those with ventilation and rainwater infiltration, can still be effectively analyzed in one dimension. As such, WUFI® 2D should be more generally thought of as a complement and not an alternative to WUFI® Pro.

#### 4.3.4 Program Setting and Inputs

The building model was generated and fed with the required input data and program settings in one and two-dimensional geometry and the position of sensors were specified in different layers of construction (Node1: interior surface, Node2: Aerogel layer, Node4: The brick wall and Node5: Exterior plaster), which illustrated in Figure 24.

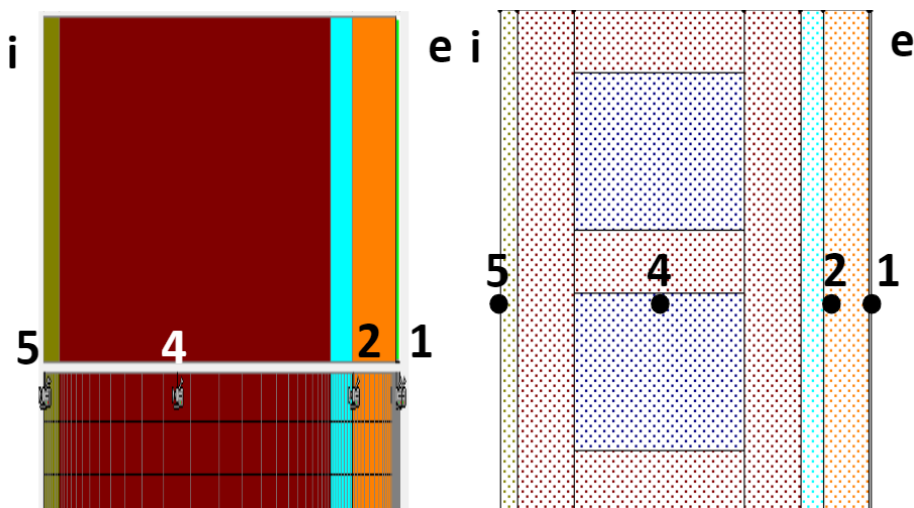


Figure 24: Layer's geometry modelled in WUFI Pro (left) and in WUFI 2D (right).

Table 5 shows the input information and settings; including the rain coefficient and surface transfer properties, together with their initial

values. The hygro-thermal and physical characteristics of the materials required for the simulations in WUFI are presented in Table 2. The properties of the materials were defined based on available information (e.g., from material catalogs), measurements and observations. In case of the missing information, the material data library of WUFI was used.

Table 5: General setting and input of WUFI (Pro – 2D)

Setting and inputs		Value	Unit
<b>Orientation</b>	Height	> 20	[m]
	Inclination	90	[°]
<b>Building height-driven rain coefficient</b>	Rain load (According to the ASHRAE Standard 160)	Rain deposition facto (FD)=1.5 Rain exposure factor (FE)=1	-
	Thermal resistance of exterior surface	0.0588	[M <sup>2</sup> ·k·W <sup>-1</sup> ]
	Sd-value of exterior surface	0.0002	[m]
<b>Surface transfer coefficient</b>	Short wave radiation absorptivity	0.2	-
	Ground short wave reflectivity	0.2	-
	Adhering fraction of rain	No absorption	-
	Thermal resistance of interior surface	0.125	[M <sup>2</sup> ·k·W <sup>-1</sup> ]
	Sd-value of interior surface	0.1	[m]

#### 4.3.5 Boundary Conditions

The boundary condition required for the simulations includes the outdoor climate and indoor environmental conditions. Software Meteonorm 7 was used (Meteonorm 2017) to create the local outdoor climate file based on the measured values from the locally installed weather station (i.e. Dry bulb temperature [°C], relative humidity [%] and Global Solar radiation [J.cm<sup>-2</sup>]). For this purpose, the software required also the dew point temperature [°C], which derived from the equation (7).

$$\theta_{dp} = \left(\frac{RH}{100}\right)^{0.125} \cdot (112 + 0.9\theta_{air}) + 0.1\theta_{air} - 112 \quad [^{\circ}\text{C}] \quad \text{Eq. 7}$$

Actual indoor environmental condition was generated by WUFI climate file creator (WAC format) base on the measured indoor air temperature

[°C], relative humidity [%], longitude [°], latitude [°] and altitude [m] of city Vienna. Moreover, the initial condition (Table 6), i.e. the temperature and water content of each layer at the beginning of the run period, must be specified as a text file to import in the WUFI software including the coordination of each node (Figure 25), initial temperature and initial moisture in component. The initial moisture (water content) for each layer was defined based on the corresponding measured relative humidity (sorption isotherm - Figure 26) by equation (8).

$$W_i - W_1 = \left( \frac{W_2 - W_1}{RH_2 - RH_1} \right) \cdot (RH_i - RH_1) \quad \text{Eq. 8}$$

Table 6: Initial conditions assumptions in the initial simulation model

Initial conditions	Unit	Exterior plaster	Aerogel	Brick	Interior plaster
Destination	[m]	0.0019	0.041	0.2034	0.3255
Temperature	[°C]	-1.88	13.37	17.05	19.18
Relative humidity	[%]	72.09	31.64	41	22.37
Water content	[kg·m <sup>-3</sup> ]	31.679	0.796	2.120	0.408

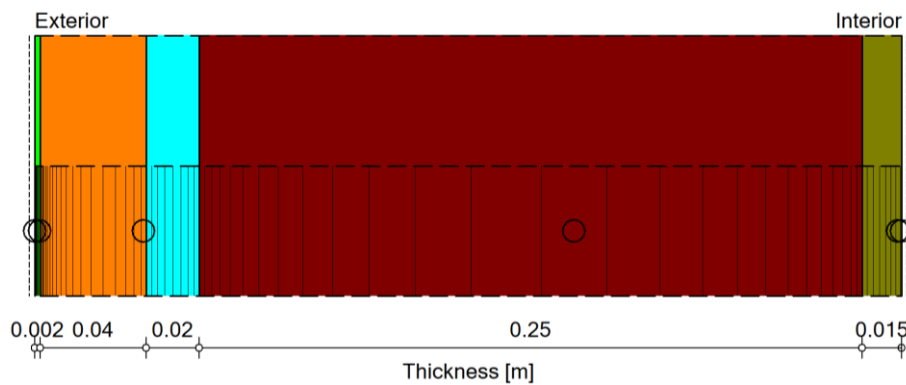


Figure 25: The monitor positions of each node according to the real condition

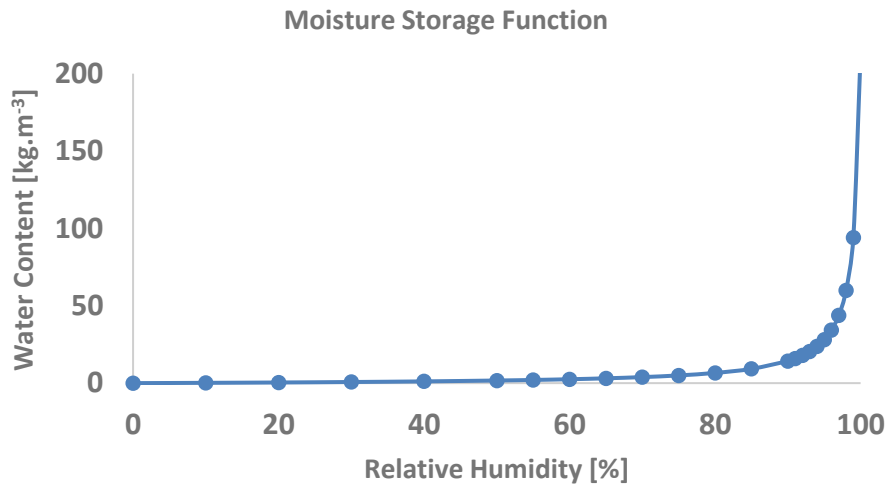


Figure 26: Aerogel- based rendering sorption curve (Ibrahim et al. 2014)

#### 4.3.6 Sensitivity Analysis

There is a very large and diverse literature on sensitivity analysis, however (Pannell 2017) express that the parameter values and assumptions of any model are subject to change and error. Sensitivity analysis (SA), broadly defined, is the investigation of these potential changes and errors and their impacts on conclusions to be drawn from the model. Sensitivity analysis is a data-driven investigation of how certain variables impact a single, independent variable and how much changes in those variables will change the independent variable. SA can be used to assess the "riskiness" of a strategy or scenario. By observing the range of objective function values for the two strategies in different circumstances, the extent of the difference in riskiness can be estimated and subjectively factored into the decision. In addition, it is a process of creating new information about alternative strategies. It allows the modelers to improve the quality of their subjective beliefs about the merits of different strategies.

##### 4.3.6.1 Model Evaluation

Model evaluation is used to assess goodness of fit between model and data, to compare different models, in the context of model selection,

and to predict how predictions (associated with a specific model and data set) are expected to be accurate. The simulated temperature and relative humidity at each layer were compared to the corresponding measured values at each time step. Errors can be calculated as the difference between the predicted values, i.e. simulation results, and the measured values. In this study, some of statistical indicators as follows were used.

#### 4.3.6.1.1 Absolut and relative Error

Absolute and relative errors are two types of errors that are affected by the accuracy of measuring tools. Absolute error is the amount of physical error in a measurement, period. It is defined, the difference between the measured value and the true value and it denoted by  $E_{abs}$  (Equation 9).

$$E_{absolut} = m_i - s_i \quad Eq. 9$$

Relative error gives an indication of how good a measurement is relative to the size of the thing being measured. That is affected by the accuracy of measuring tools. It denoted by  $E_{rel}$  and it defines absolute error divided by the magnitude of the measured value (Equation 10).

$$E_{relative} = \frac{m_i - s_i}{m_i} \quad Eq. 10$$

#### 4.3.6.1.2 Coefficient of variation of Root-mean-square deviation CV (RMSD):

The RMSD represents the sample standard deviation of the differences between predicted values (simulated values) and observed values (measured values). These individual differences are called residuals when the calculations are performed over the data sample that was used for estimation, and are called prediction errors when computed out-of-sample. The RMSD serves to aggregate the magnitudes of the errors in predictions for various times into a

single measure of predictive power it is also a good measure of accuracy, but only to compare forecasting errors of different models for a particular variable and not between variables, as it is scale-dependent. The CV (RMSD) is an aggregates time step errors over the runtime into a single dimensionless number.

$$RMSD = \sqrt{\frac{\sum_{i=1}^n (m_i - s_i)^2}{n}} \quad Eq. 11$$

$$(CV)RMSD = \frac{RMSD}{\bar{m}} \cdot 100 \quad Eq. 12$$

#### 4.3.6.1.3 Coefficient of determination R-squared

R-squared is a statistical measure of how close the data are to the fitted regression line. It is also known as the coefficient of determination, or the coefficient of multiple determinations for multiple regressions. The R-squared it is the percentage of the response variable variation that is explained by a linear model.

R-squared is always between 0 and 100%:

- 0 % indicates that the model explains none of the variability of the response data around its mean.
- 100 % indicates that the model explains all the variability of the response data around its mean.

Additional, the coefficient of determination  $R^2$ , which describes the proportion of the variance in measured data explained by the model (Tahmasebi and Mahdavi 2013).

$$R^2 = \left( \frac{n \sum m_i s_i - \sum m_i \sum s_i}{\sqrt{(n \sum m_i^2 - (\sum m_i)^2) \cdot (n \sum s_i^2 - (\sum s_i)^2)}} \right)^2 \quad Eq. 13$$

In Equations 9 to 13,  $m_i$  is the measured data at each time step,  $s_i$  is simulated data at each time step,  $n$  is the total number of time steps, and  $m$  is the mean of the measured values.

#### 4.3.6.1.4 Cumulative percentage

The cumulative percent is the sum of all the percentage values up to that category, as opposed to the individual percentages of each category. It includes two parts as below:

- Input data is the data that would be to analyze by using the Histogram tool.
- Bin numbers represent the intervals that should be the Histogram tool to use for measuring the input data in the data analysis. It must be entered in ascending order.

#### 4.3.6.2 Selecting Calibration Variables via Sensitivity Analysis

In order to identify the impact of these uncertainties on simulation results, a sensitivity analysis can be performed (Eisenhower et al. 2012). In this order a subset of the input variables most likely to influence the simulation results, first, the large number of candidate model parameters was reduced to a certain extent via heuristically-based considerations. This subset included 18 model input variables (Table 7). Secondly, these variables were subjected to a sensitivity analysis.  $R^2$ , RMSD and (CV) RMSD of temperature and relative humidity were calculated for the variables as a quantitative sensitivity measure in comparison with measured data as a base case quantitative sensitivity measure.



Table 7: Variables subjected to SA and their ranges Variables

	Sensitive parameters	Benchmark Model	Possible Values		
Material Properties	Basic	Bulk density [kg.m <sup>3</sup> ] of Aerogel	220	146	
		Bulk density [kg.m <sup>3</sup> ] of Brick	1560	765	
		Porosity [m <sup>3</sup> .m <sup>-3</sup> ] of Aerogel	0.92	0.98	
		Porosity [m <sup>3</sup> .m <sup>-3</sup> ] of Brick	0.38	0.60	
	Hygro-Thermal	Reference water content [kg.m <sup>-3</sup> ]	6.6	12.5	
		In relative humidity 80% _ Aerogel			
		Reference water content [kg.m <sup>-3</sup> ]	11.8	13	
		In relative humidity 80% _ Brick			
		Free water saturation [kg.m <sup>-3</sup> ]			
		In relative humidity 80% _ Aerogel	213	150	
		Free water saturation [kg.m <sup>-3</sup> ]			
		In relative humidity 80% _ Brick	368.96	193	
		Water absorption coefficient [kg.m <sup>-2</sup> s <sup>-0.5</sup> ] (A-Value) _ Brick	0.583	0.16	
		Exterior surface properties	Sd-Value of exterior surface	0.0002	Stucco.Acrylic
			1.00	0.20	
Short wave radiation absorptivity	Stucco.white 0.20		No absorption	Stucco.normal 0.40	
Ground short wave reflectivity	Standard value 0.20		No reflection	Light building surface 0.60	
Adhering fraction of rain	No absorption		Depending on inclination of component		
Rain load calculation	ASHRAE standard 160 FE=1.5 FD=1		Rain×(R1+R2+wind velocity)		
Climate	Indoor climate	EN15026	EN13788	ASHRAE 160 Measured data	
	Outdoor climate	Map file	Local created weather data		
Initial conditions		Constant across component	In each layer	Measured data	

Figure 27 and Figure 32 shows the analysed variables in order to explore the potential of the sensitive variables. Based on these results, three

variables, which have  $R^2$  values higher than 0.6, were chosen to be subjected to optimization-based calibration in the next stage. These variables, their initial values and their allowed calibration ranges can be seen in table x.

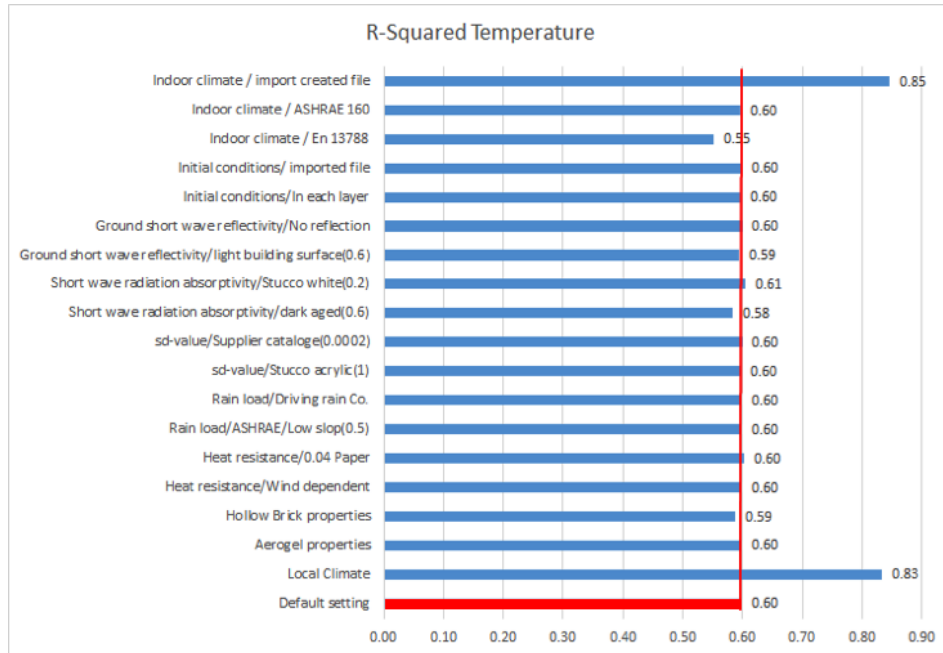


Figure 27:  $R^2$  –Value of temperature of analysed variables

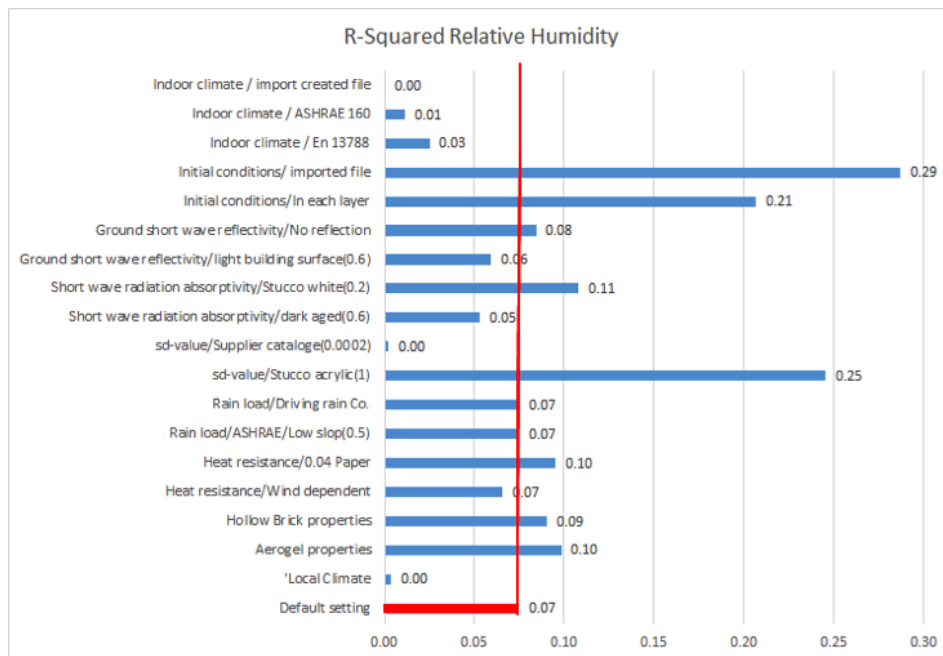


Figure 28:  $R^2$  –Value of relative humidity of analysed variables

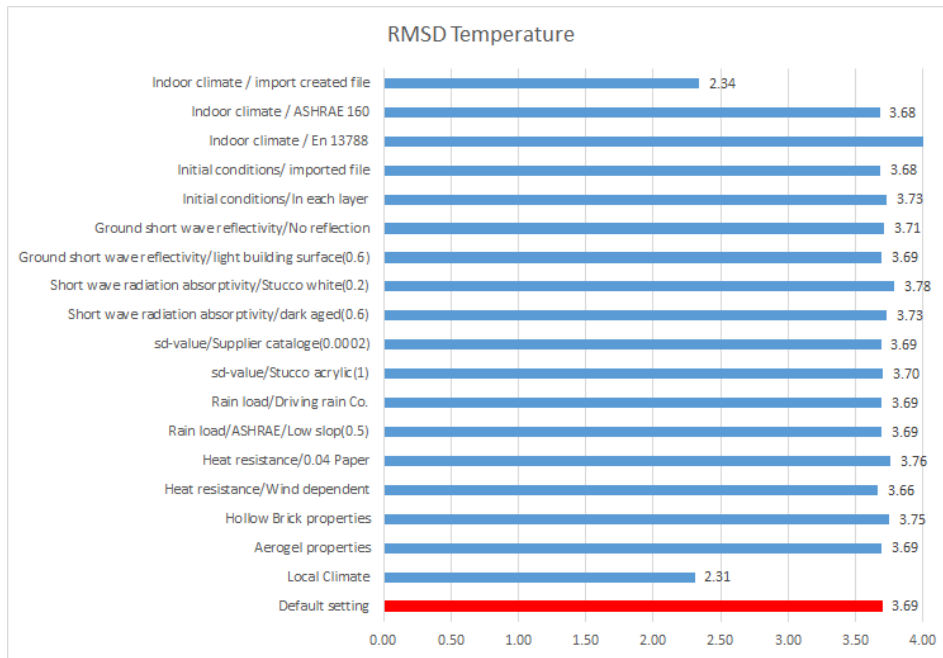


Figure 29: RMSD –Value of temperature of analysed variables

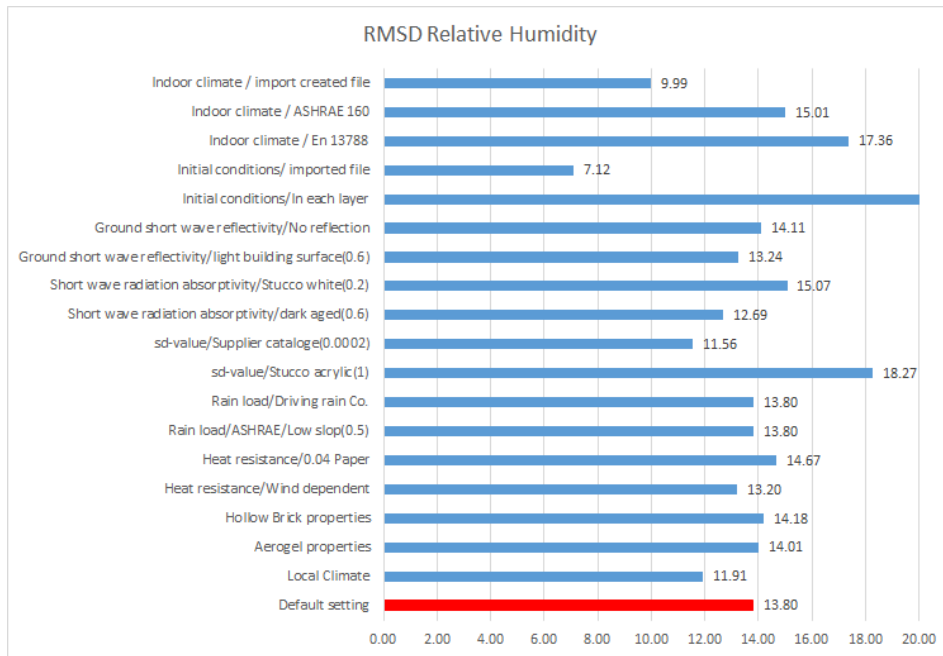


Figure 30: RMSD –Value of relative humidity of analysed variables

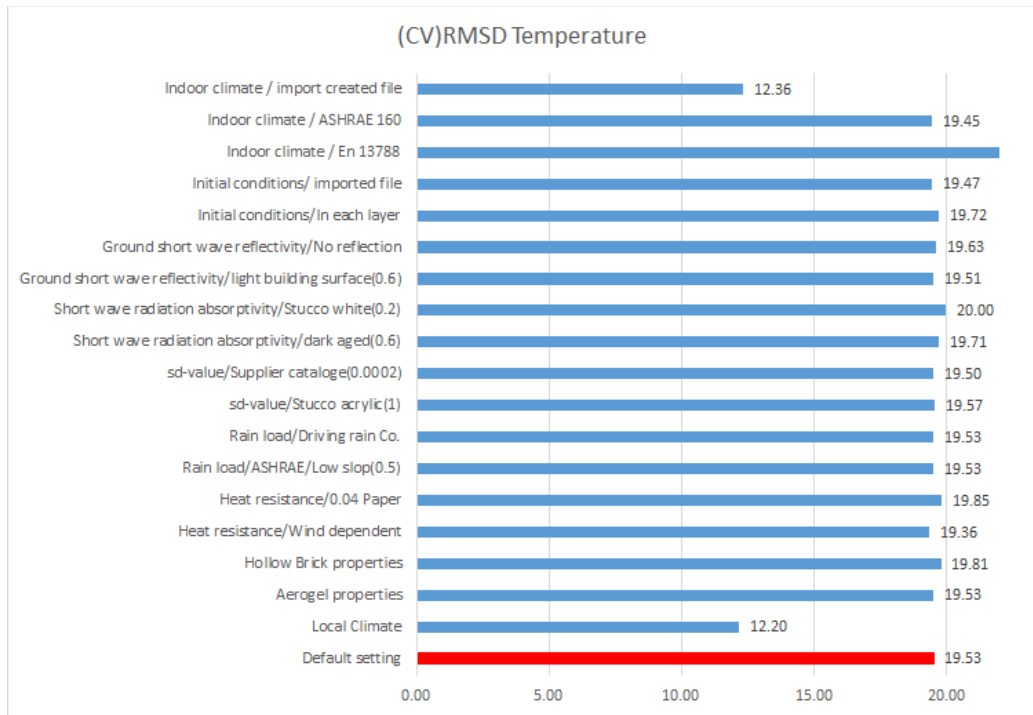


Figure 31: (CV) RMSD –Value of temperature of analysed variables

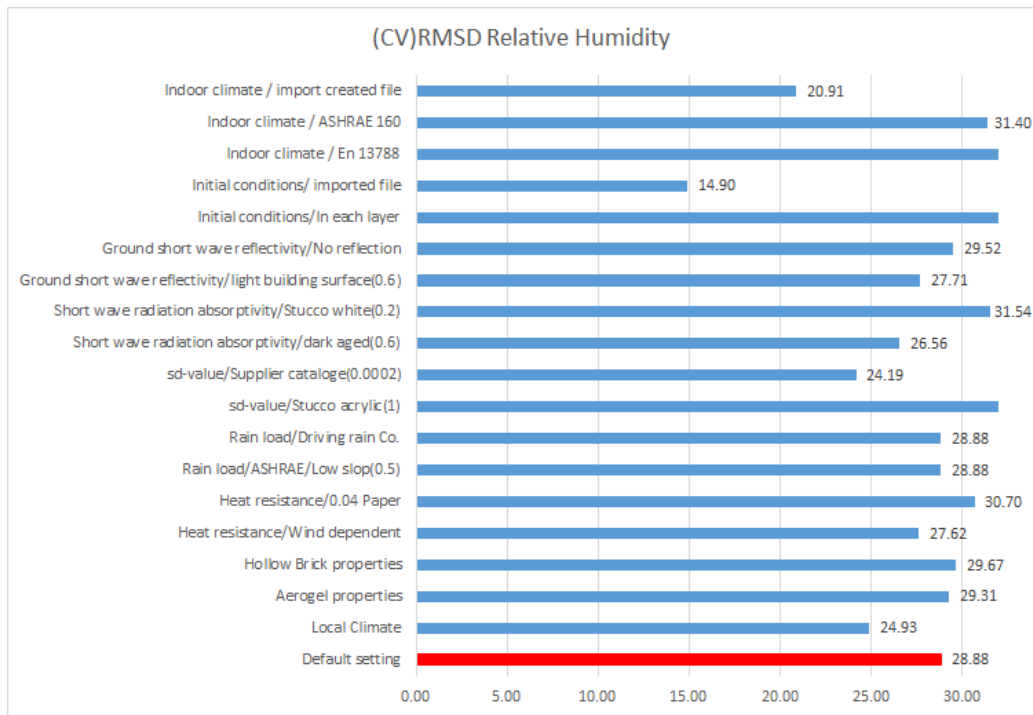


Figure 32: (CV) RMSD –Value of relative humidity of analysed variables

#### 4.3.7 Calibration

To increase the credibility of the simulation outcomes, calibration of the initial energy performance simulation models, assisted by monitored data, has been presented as a promising method (Reddy 2006). Measured data was used to define the model's initial conditions and to evaluate the validity of the simulation results. Furthermore, the study explores the impact of input assumptions, i.e. boundary conditions, and layers' geometry modeling techniques (one versus two-dimensional), on the rate of accordance between the measured and simulated performance indicators' values. The results displayed that the predictive potency of the simulation model can considerably improve by adjusting the input variables based on measurements. Moreover, more dependable simulation results were achieved as a result of the more detailed representation of the component's geometry.

##### 4.3.7.1 Simulation Scenarios

Scenarios were designed based on alternative configurations of input data (i.e. initial condition, indoor and outdoor climate, layers' geometry) to explore the reliability of hygro-thermal simulation models and potential model calibrations. These configurations (labeled as Initial Model, Scenario 1, Scenario 2, Scenario 3, and Scenario 4) are listed in Table 8. Note that, general setting and material properties presented in the Table 2 and Table 5 were kept constant in all configurations.

**Initial model:** Initial conditions in this model were the default values suggested by the program (temperature 20°C and relative humidity 80% for each layer). The outdoor climate was selected from the database of WUFI for the city of Vienna, Austria. Indoor climate was automatically derived in the program based on outdoor climate, by using standard EN15026 (EN15026 2007) recommended by WUFI.

**Scenario 1:** Similar to the initial model, however in this case the initial condition for each layer was defined based on the measured data. In

fact, the initial conditions were imported as a text file including measured values at the beginning of the run period.

**Scenario 2:** Similar to Scenario 1, with the imported actual indoor environmental conditions, instead of the calculated indoor conditions.

**Scenario 3:** An outdoor climate file was created based on the measured values from the locally installed weather station. Software Meteonorm 7 was used for this purpose (Meteonorm 2018).

**Scenario 4:** To evaluate the impact of detailed modeling of the component's geometry on simulation predictions WUFI 2D was used in this Scenario instead of WUFI Pro (Figure 33). All other input assumptions were kept exactly the same as in Scenario 3.

Table 8: Simulation Scenarios

Simulation scenarios	Initial conditions	Indoor conditions	Outdoor climate	WUFI
<b>Initial model</b>	Constant software default values equal for all layers	Calculated by software using EN15026 [9]	Reference Vienna weather file	Pro
<b>Scenario 01</b>	Measured values for each layer	Calculated by software using EN15026	Reference Vienna weather file	Pro
<b>Scenario 02</b>	Measured values for each layer	Measured Indoor climate	Reference Vienna weather file	Pro
<b>Scenario 03</b>	Measured values for each layer	Measured indoor climate	Local weather file Vienna	Pro
<b>Scenario 04</b>	Measured values for each layer	Measured indoor climate	Local weather file Vienna	2D

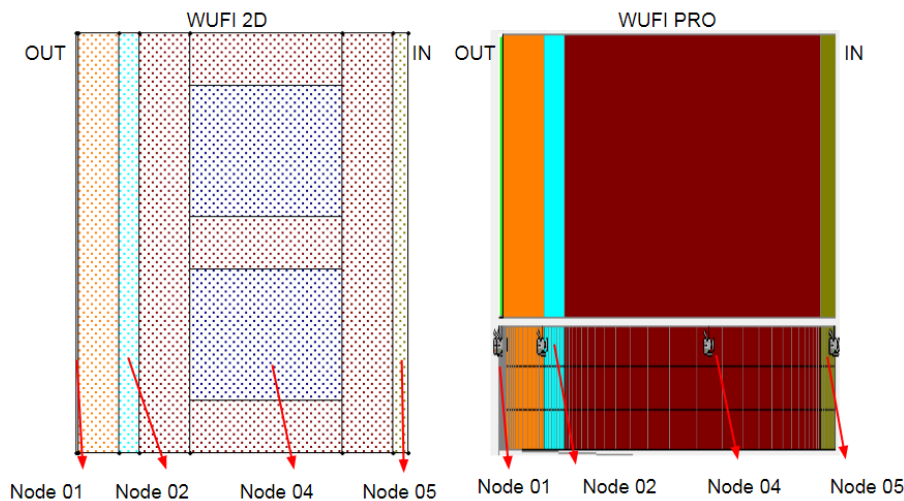


Figure 33: Layer's geometry modelled in 2D (left), and WUFI Pro (right)

#### 4.4 Evaluation Method

The simulation results of the hygro-thermal performance indicators, namely temperature and relative humidity, were compared with the corresponding measured values at each time step. For a better comparison, four statistical indicators were used. The first measure is the coefficient of variations of root mean squared deviations CV (RMSD), which aggregates time step errors over the runtime into a single dimensionless number. Moreover, the coefficient of determination  $R^2$  was used, which describes the proportion of the variance in measured data explained by the model (Tahmasebi and Mahdavi 2013). In addition, the absolute and relative errors were calculated for each scenario in this study.

#### 4.5 Result and Discussion

Figure 34 and Figure 35 respectively present the distribution of relative humidity and temperature in each node in different simulation scenarios as well as measurements. Based on these results through the simulation scenarios, the relative humidity in nodes 2, 4, and 5, (aerogel, brick, and interior plaster, respectively) improved significantly and became closer to the measurements. The temperature results illustrate some improvement in all nodes.

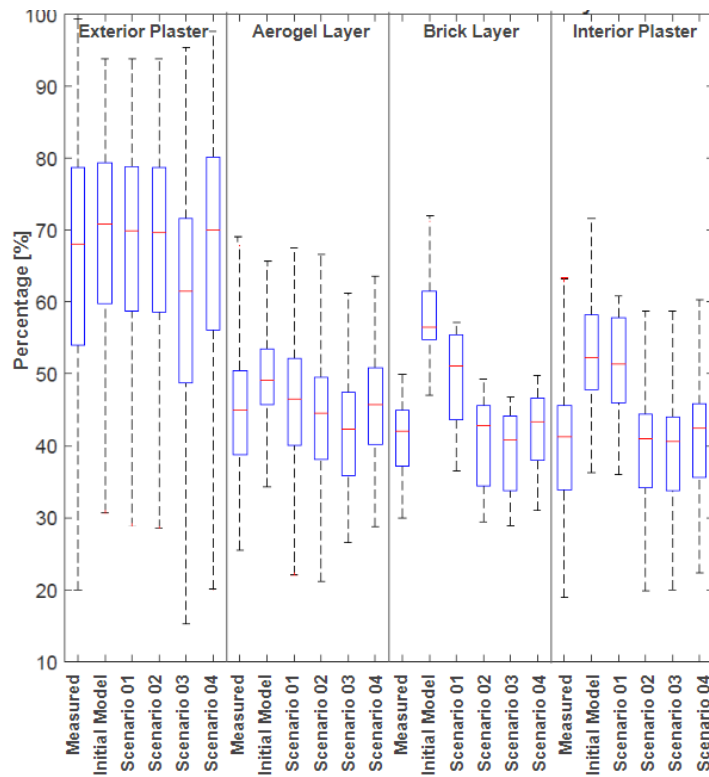


Figure 34: Distribution measured relative humidity in all scenarios and each node

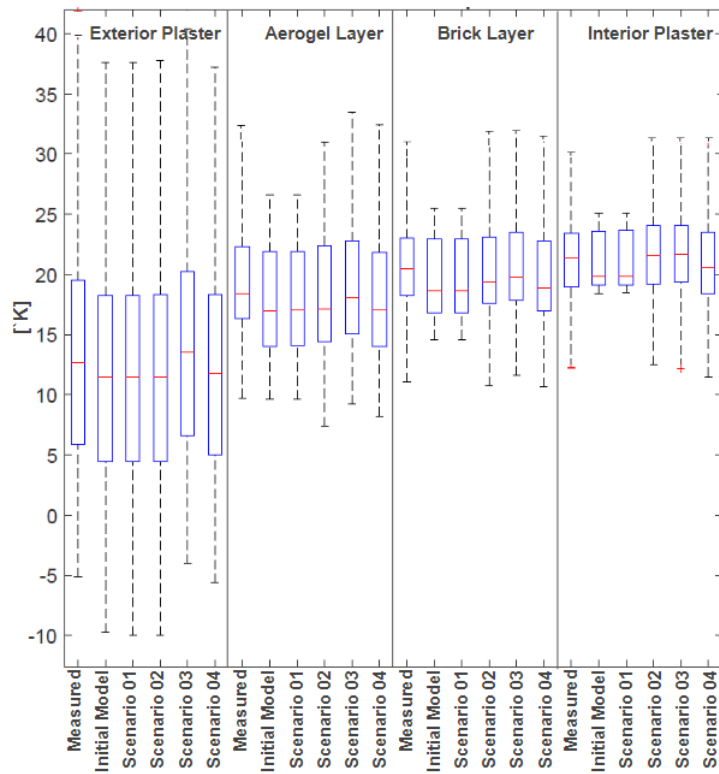


Figure 35: Distribution measured temperature in all scenarios and each node



Figure 36 show the  $R^2$  values of relative humidity and temperature of all scenarios in each node, respectively. The model in scenario 3 generated outputs with acceptable  $R^2$  values, for both relative humidity (more than 0.8) and temperature (more than 0.94). There was a significant improvement after feeding in the actual indoor conditions (Scenario 2), in three layers of Aerogel, brick, and interior plaster. Moreover, feeding the local outdoor climate (Scenario 3) improved the result of relative humidity and temperature in the exterior plaster layer.

Detailed modeling of the layer's geometry (Scenario 4) was slightly effective in improving  $R^2$  values for relative humidity. However, temperature values appear not to be sensitive to detailed geometry modeling in our case.

Figure 37 illustrates the calculated CV (RMSD) for each node in the corresponding scenarios. The calculated errors are below 10% and 5 K for relative humidity and temperature, respectively, except in node 01, which shows higher corresponding errors (13% and 15 K).

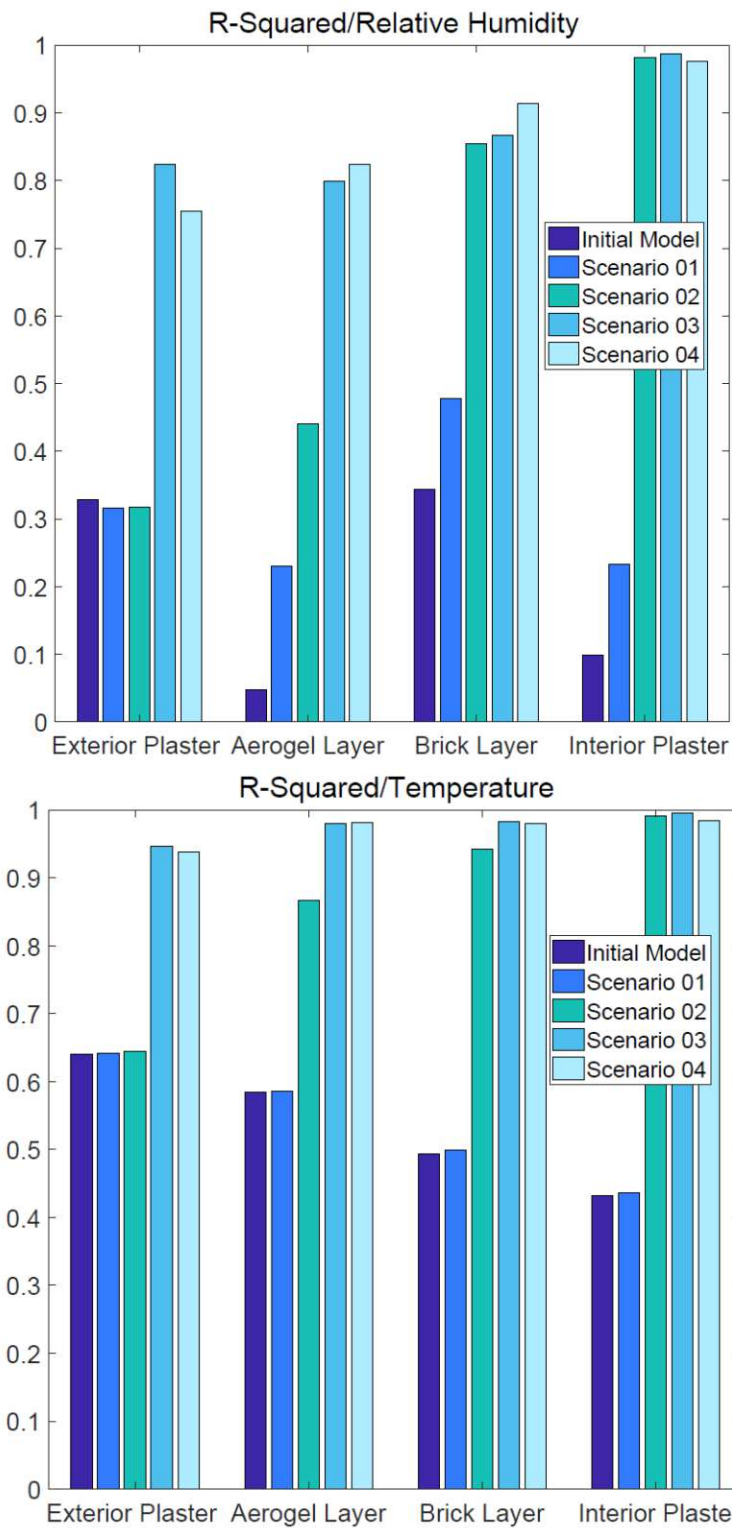


Figure 36:  $R^2$  of relative humidity (left) and temperature (right) of all scenarios in each node

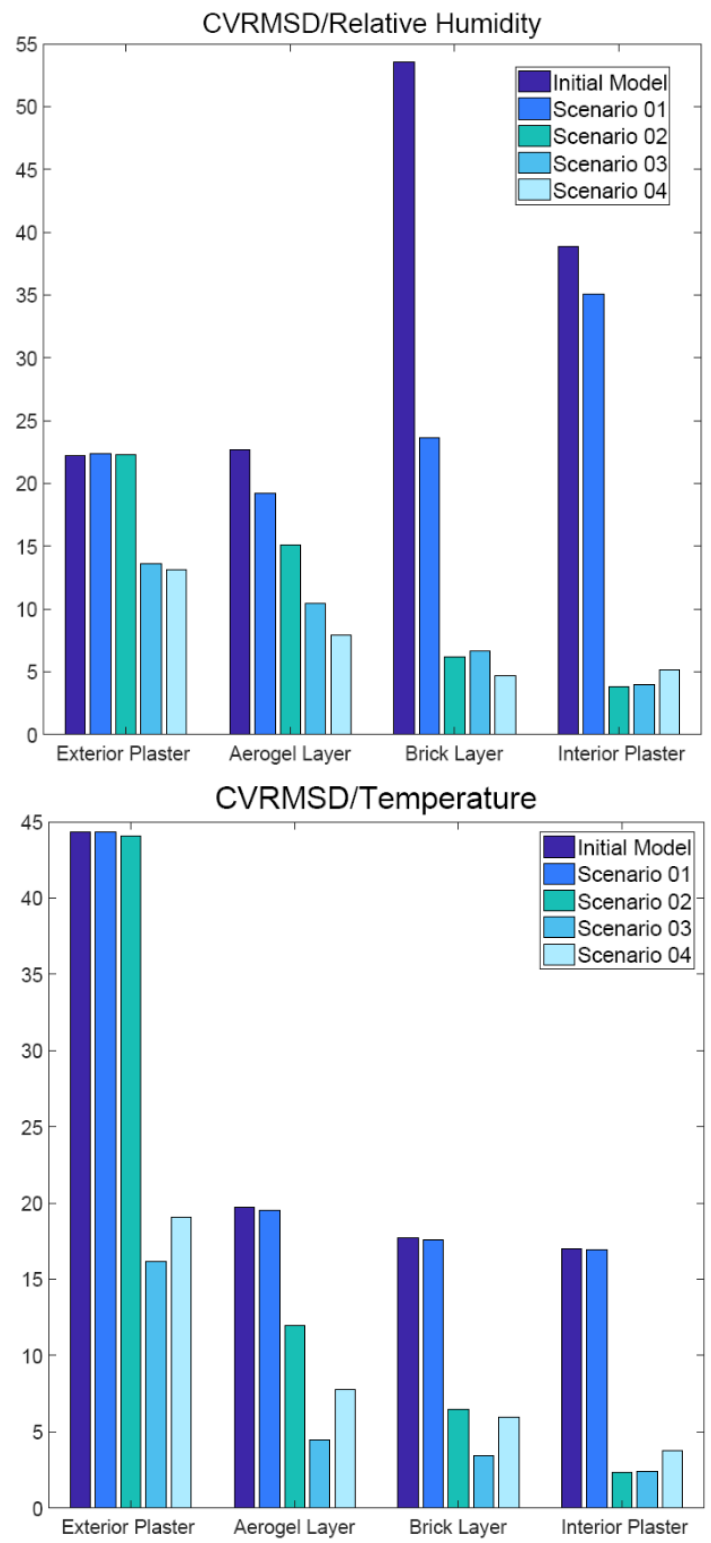


Figure 37: (CV) RMSD of relative humidity (left) and temperature (right) of all scenarios in each node

The calculated absolute and relative errors (see, Figure 38 to Figure 43) further confirm the above-mentioned results. Calculated absolute errors of less than 1K for the temperature and 5% for the relative humidity show considerable improvements in all nodes (Figure 38Figure 39). The rate of errors in exterior layer is slightly higher as compare to the other layers (i.e. 2K and 8% for temperature and relative humidity, respectively).

A similar pattern of improvement was observed in relative errors. Figure 43-40 indicate the cumulative percentage of relative errors for relative humidity in all nodes. Note that, except for the interior plaster layer, Scenario 4 (modeled in WUFI 2D) has the minimum rate of relative error in all nodes. Scenario 4 especially performs better in the Aerogel and brick layer. In case of the interior plaster layer, Scenarios 2 and 3 were more effective. As shown in Figure 44, detailed geometry modeling of hollow brick, namely two-dimensional modeling, improved the relative humidity predictions.

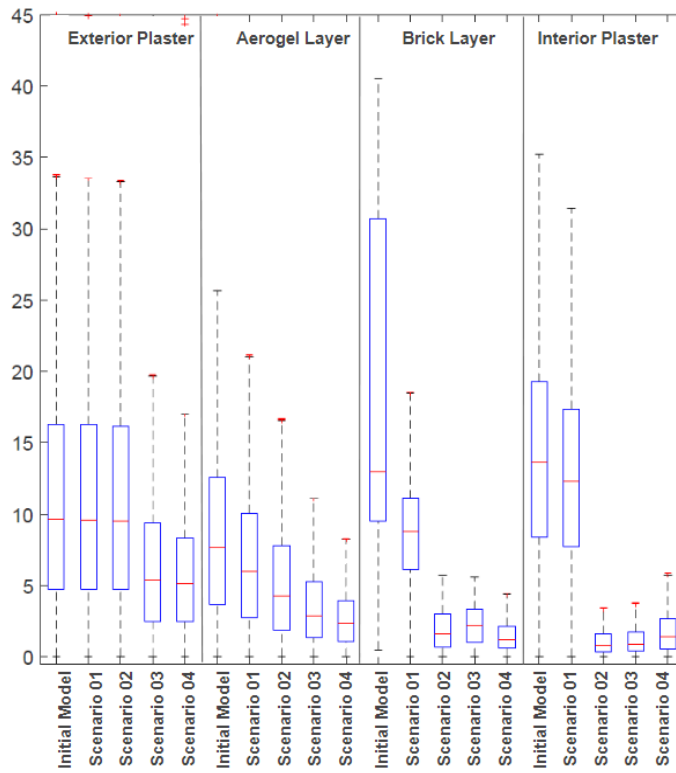


Figure 38: Absolute error of relative humidity [%] of all scenarios for each node

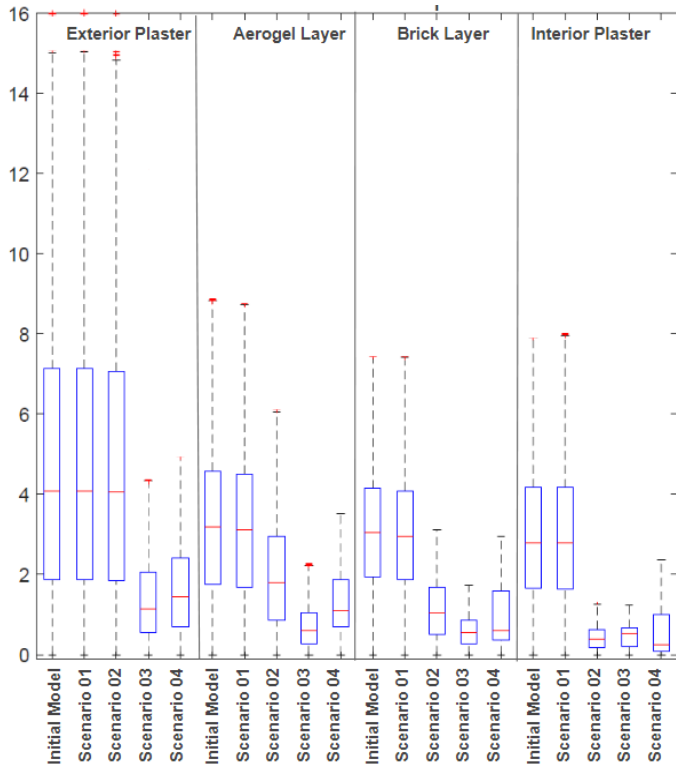


Figure 39: Absolute error of temperature [K] of all scenarios for each node

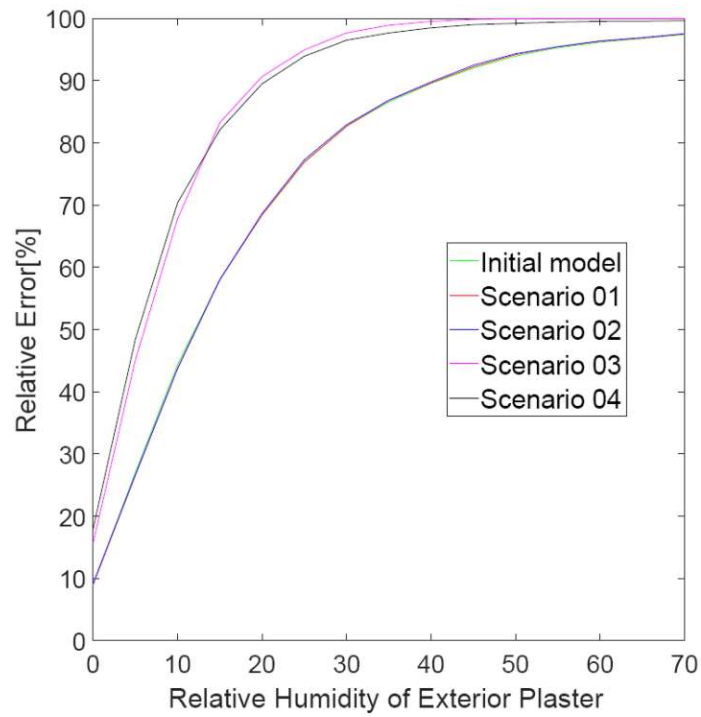


Figure 40: Relative error of relative humidity of exterior plaster

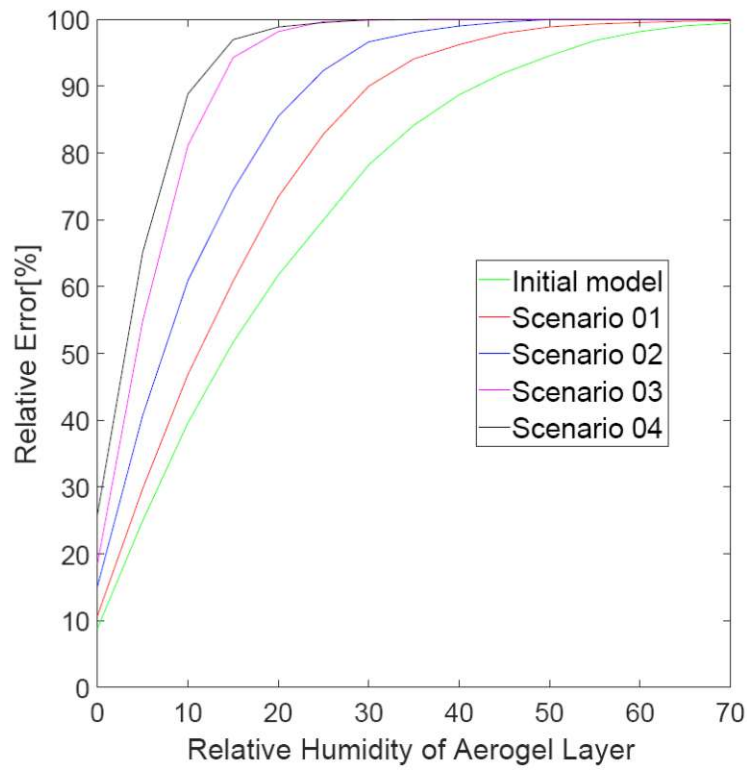


Figure 41: Relative error of relative humidity of Aerogel layer

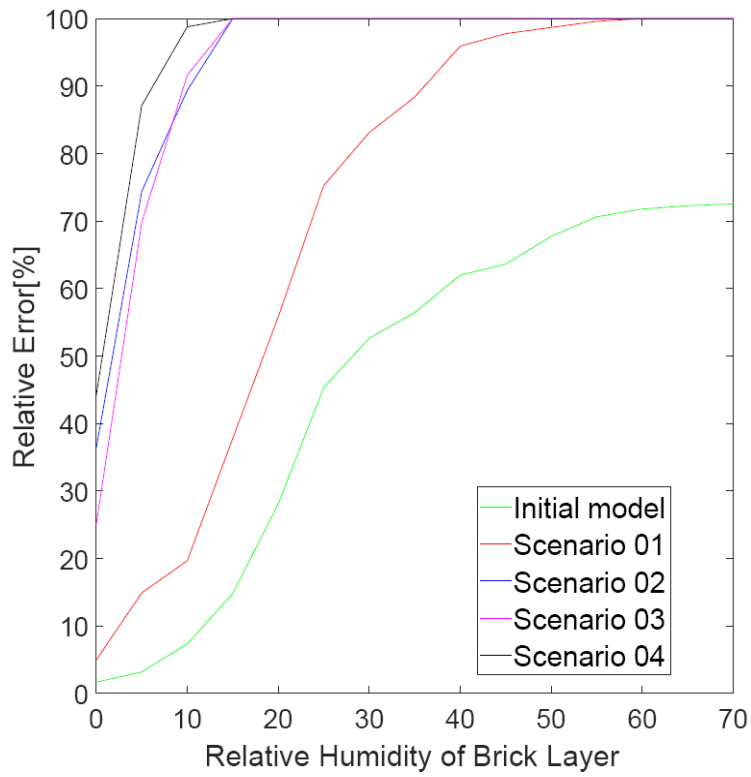


Figure 42: Relative error of relative humidity of Brick layer

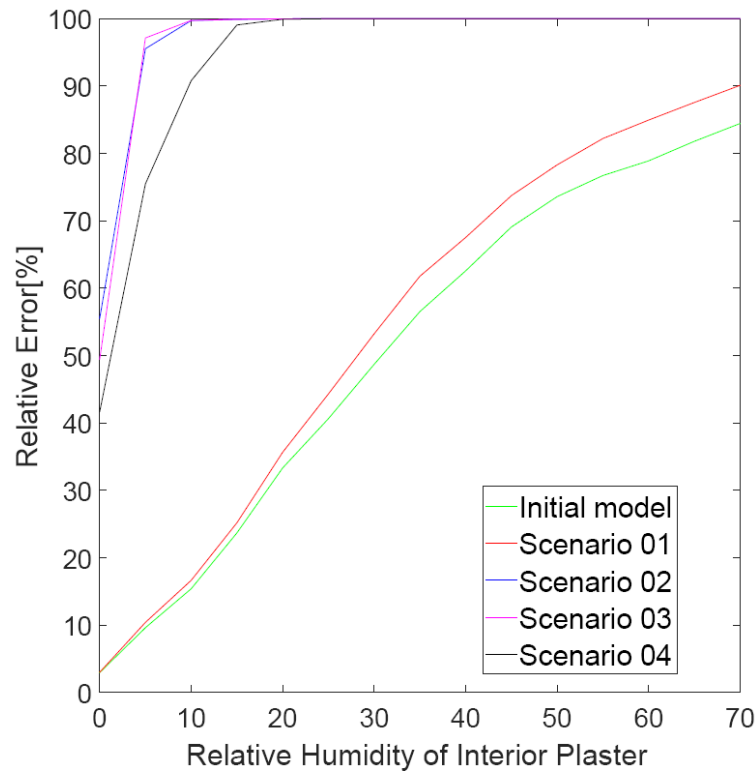


Figure 43: Relative error of relative humidity of Interior plaster

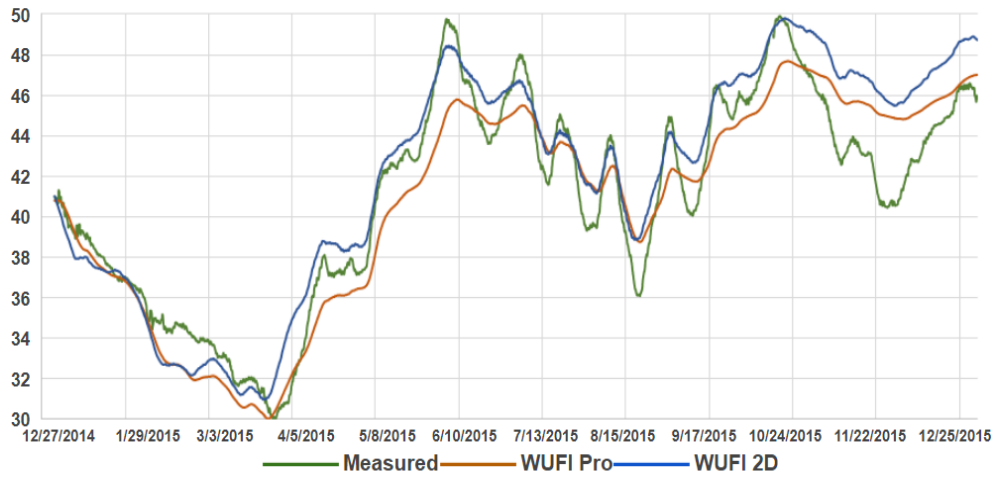


Figure 44: Trend of relative humidity in middle of the wall-Brick layer



## CHAPTER 5.


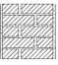

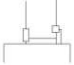
### EVALUATION OF THICKNESS AND LOCATION OF INSULATION LAYER IN WALL CONFIGURATION

Application of insulation to external walls can represent an effective measure (Xin et al. 2018). However, a considerable fraction of existing building facades in Europe must be protected in view of historical significance. Moreover, the risk of interstitial condensation resulting from improper thermal retrofit can lead to undesirable consequences (Ibrahim et al. 2014). In this regard, effective moisture control can reduce condensation risk and contribute to energy use reduction (F. Pacheco Torgal et al. 2016). Insulating plaster-based materials involving silica aerogels could represent a potential solution for thermal retrofit of facades, whose original appearance must be preserved (Schuss et al. 2017). Respective solutions must address both energy use reduction and moisture control via consideration of the characteristics and configuration of the insulating system (e.g., locations of insulation layers, insulation thickness)(Ozel 2014)(Stahl et al. 2012). Such solutions can be assessed proactively using appropriate software (Mundt Petersen and Harderup 2013). For the purpose of the present contribution, a typical Austrian residential building was selected as a case study to investigate the effect of aerogel plaster position (specifically, inside versus outside) and thickness (from 3 to 10 cm) on the thermal and hygro-thermal performance by using a hygro-thermal simulation model. One set of results pertains to the influence of insulation on energy use. We specifically considered variables pertaining to heating and cooling loads compared to the reference case (façade with conventional plaster). A second set of result suggests that the position of aerogel plaster noticeably influences the condensation and mould growth risk in the winter period. Specifically, exterior positioning leads to a preferable performance.

### 5.1.1 Case Study

To examine annual energy demand (HWB) as performance indicator, a typical multi-unit apartment building in the city Vienna, Austria was selected as a base case. Figure 45 shows the typical plan and section of this building. The building has two blocks (A and B) in six floors, connected via staircase and corridors in Habichergasse20, Vienna. The attic space of block B and basement of block A are unheated. The building entails residential units with a total net heated space area of 1737 m<sup>2</sup>. The assumed data on the building's construction in **Fehler! Verweisquelle konnte nicht gefunden werden.** were assumed based on its construction date (TABULA 2018). The existing wall construction of the case study (with three layers including gypsum plaster, solid brick masonry and lime cement plaster), was assumed to be retrofitted by applying a solution encompassing the highly insulating Aerogel layer Fixit 222 (2018). Table 2 presents the assumed hygro-thermal characteristics of the component layers.

Table 9: Construction data on Austria building types

Elements	Roof	Wall	Floor	Window
Schematic				
U-Value [W.m <sup>-2</sup> . k <sup>-1</sup> ]	0.08	1.10	0.71	2.20
Construction	Wooden ceiling with filling, wooden planks	Solid brick wall	Brick vault ceiling	Single glazing box

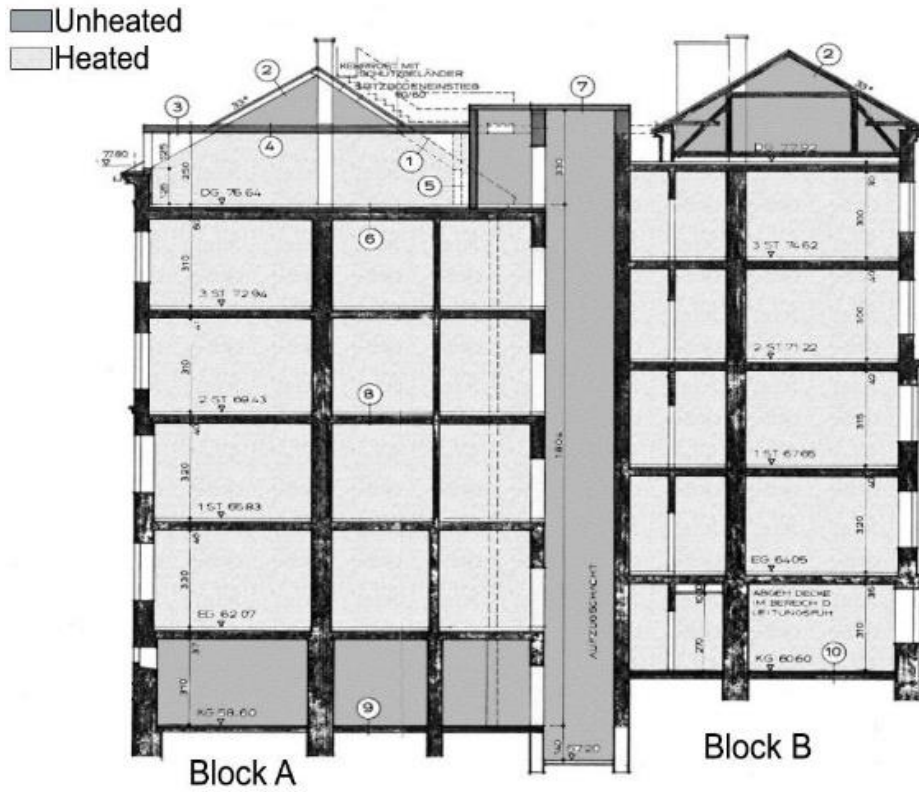
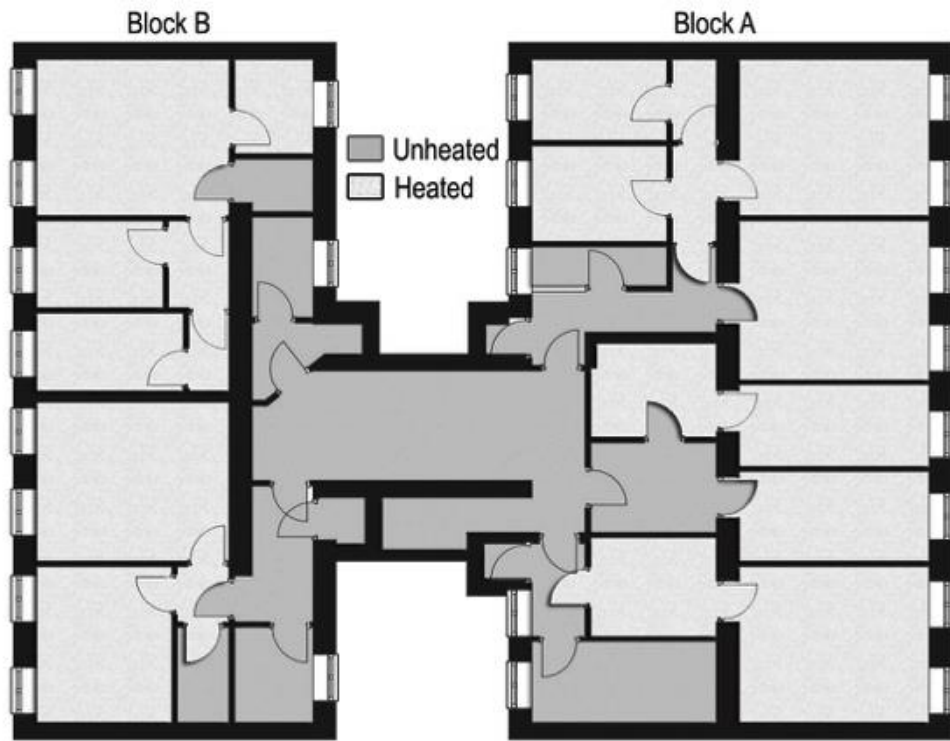


Figure 45: Plan and Section thermal zoning of the case study building model

### 5.1.2 Simulation Tool

Energy Plus™ is a whole building energy simulation program that engineers, architects, and researchers use to model both energy consumption for heating, cooling, ventilation, lighting and plug and process loads and water use in buildings. The base simulation model is created according to current construction details, materials, and systems in the case regions in Sketch up software - Open studio, which plug in on Sketch Up program helps to apply the thermal conditions of zones and surfaces, in order to import to energy simulation programs

Figure 46

The purpose of creating a base model is to estimate the annual energy consumption of conventional construction practice for the case study project without retrofit. The building was modeled in Energy Plus v8.7.0 (2018). Equipment, occupancy and lighting schedule derived from the schedule's library of the program. The air change rate was assumed to be 0.5 [h<sup>-1</sup>]. As the second step to evaluate effect of insulation position in the layer of construction on moisture transfer, the external wall construction was modeled in WUFI Pro v5.3 (2018). The inputs and settings were defined base on previous calibrated simulation model.

### 5.1.3 Simulation scenarios

Multiple retrofit solutions for external wall were defined based on insulation thickness (3, 5, 7, and 10 cm) and position (inside vs. outside). To evaluate the hygro-thermal performance of retrofitted building model, eight scenarios were designed based on alternative configurations of thickness and position of insulation layer. These configurations were labeled as Scenario A1 to Scenario D2, as listed in Table 10.

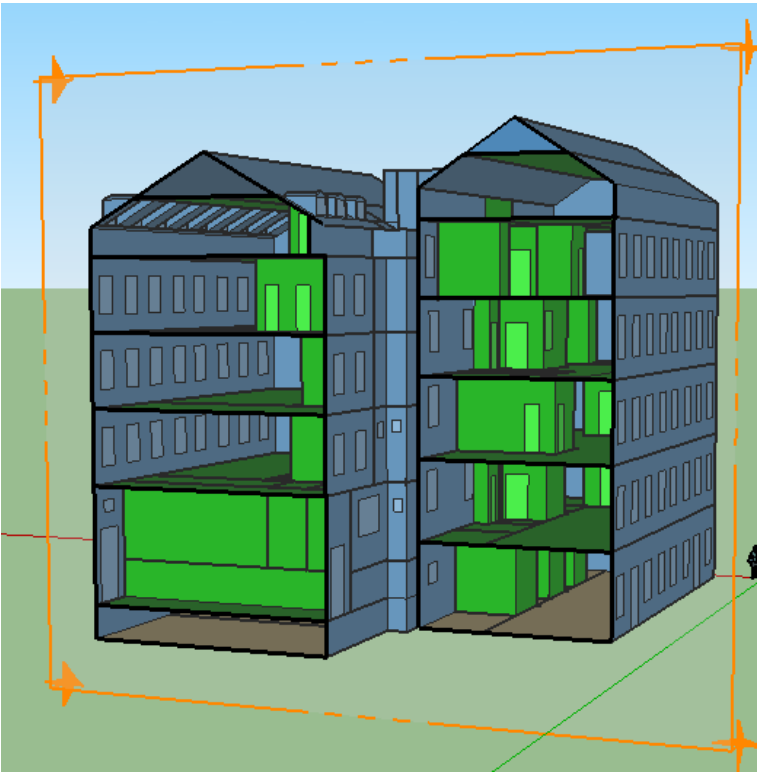
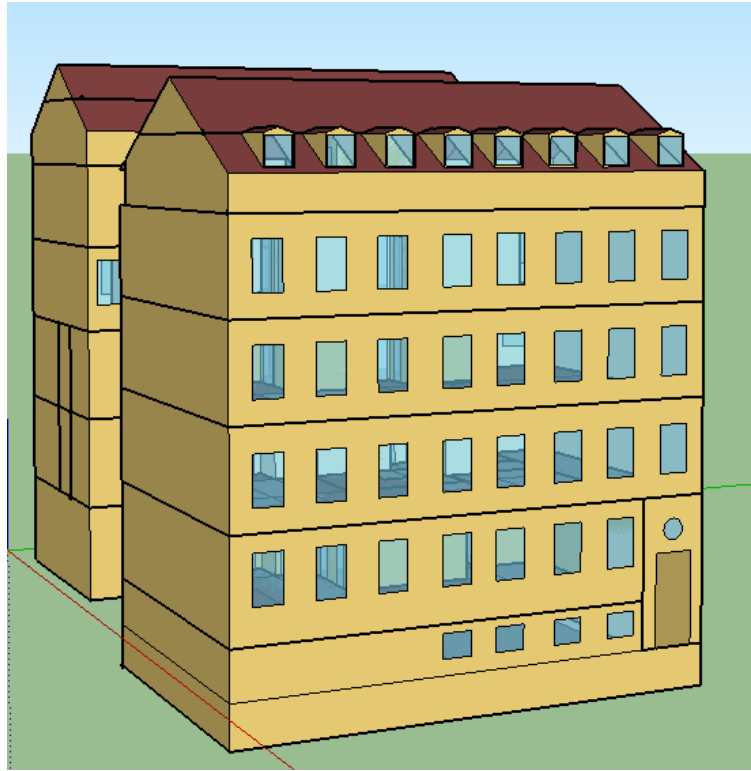


Figure 46: 3D modelling in Sketch up- Open studio to import to energy-pulse software

Table 10: *Retrofit scenarios*

Scenarios	Aerogel Thickness (m)	Aerogel Position
Base case	-	-
A1	0.03	Outside
A2	0.03	Inside
B1	0.05	Outside
B2	0.05	Inside
C1	0.07	Outside
C2	0.07	Inside
D1	0.10	Outside
D2	0.10	Inside

It should be noted that, general simulation settings and material properties were kept constant in the aforementioned configurations.

#### 5.1.4 Performance criteria

Two types of criteria were considered in the framework of this retrofitted project by applying aerogel plaster:

- Building energy (heating and cooling) demand as a function of insulation thickness
- Moisture transfer and condensation risk as a function of the position of the insulation layer

It is well known that the heat transmission load declines with increasing insulation thickness, however, the reduction rate of heating loads as the thickness increases, will be a significant challenge to achieve the optimize thickness. From this aspect, the rate of changing heating and cooling loads, which derived from energy plus simulation tool, were investigated. To assess hygro- thermal behaviour of the wall structure, condensation risk and mould growth potential, aforementioned scenarios (Table 10) were evaluated using WUFI simulation program. In this purpose, the hourly total water content values of different construction configurations (Table 2 presents the assumed hygro-thermal characteristics of the component layers.) over a period of three years (offered by the software) were analysed. Their initial water content corresponds to software settings at 20 °C and 80% relative humidity. Moreover, condensation risk assessment in middle of the wall

structure was conducted by comparing the brick layer temperature and respective dew point temperature over a period of three years for all scenarios.

### 5.1.5 Result and discussion

The simulated annual heating demand for the base case amounts to 115 kWh.m<sup>-2</sup>, which is similar to the TABULA project value (109 kWh.m<sup>-2</sup>) given for a building of this category (multifamily apartment) and age. Figure 47 illustrates the monthly heating loads (months without heating load are excluded) for the base case model and various insulation thickness values (scenarios A1, B1, C1, and D1).

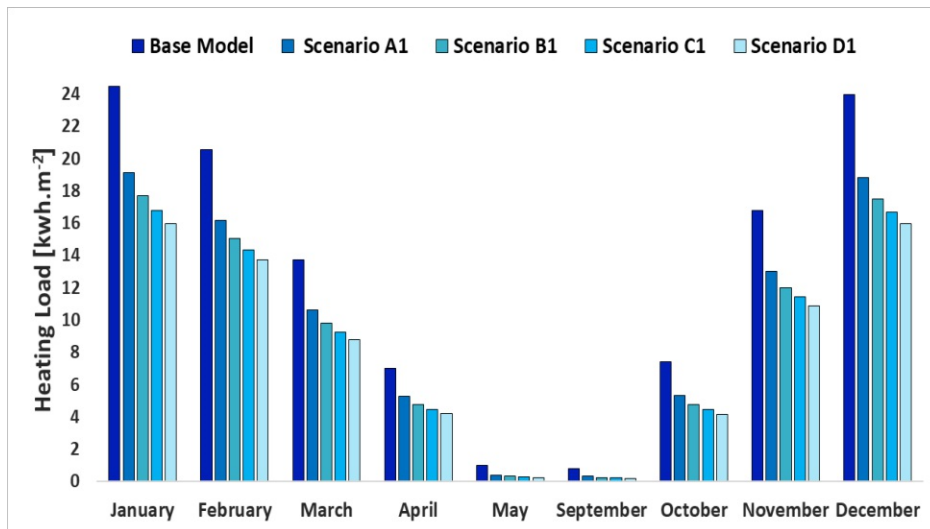


Figure 47: Comparison of the simulated scenarios (see Table 10) in terms of the resulting monthly heating loads (months without heating load are excluded)

As it can be seen, in January and December (peak demand of heating load), scenario A1 (applying 3 cm thickness of insulation plaster) leads to a 21% reduction of heating load, while the rate of decrease drops down to 6, 4, and 2% as the insulation thickness increases in scenario B1 (5 cm), C1 (7 cm), and D1 (10 cm). Annual heating and cooling reduction for various insulation thickness values (scenarios A1, B1, C1, and D1) are compared to the base model in Table 11. Whereas the heating load

reduction potential is noteworthy (23 - 36%), cooling loads are only slightly reduced with increased insulation thickness (scenario A1– D1).

Table 11: Annual heating and cooling reduction (as compared to the base model) for various insulation thickness values (scenarios A1, B1, C1, and D1)

Scenarios	A1	B1	C1	D1
Heating load	23%	29%	33%	36%
Cooling load	3%	2%	1%	-0.5%

Figure 48 shows the total amount of water content for different construction configurations over a period of three years. Thereby, the influence of the assumed initial conditions on the early phase of the simulation period can be seen. The results suggest that the total water content values of the wall structures were significantly higher when the insulation layer is positioned inside (scenario A2-D2) rather than outside (scenario A1-D1), especially in the winter period.

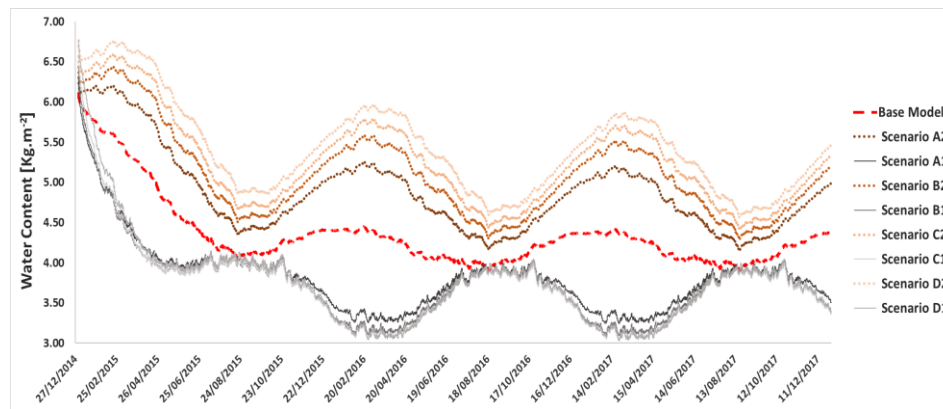


Figure 48: Simulated whole construction water content over a period of three years for different configurations

Figure 49 to Figure 51 show the brick layer temperatures and corresponding dew point temperatures for the base model, scenario B2 (insulation positioned inside), and B1 (insulation positioned outside). As it can be seen from these figures, in case of B1, condensation is unlikely. However, it can occur in case of B2, and to a lesser extent, in the base case.



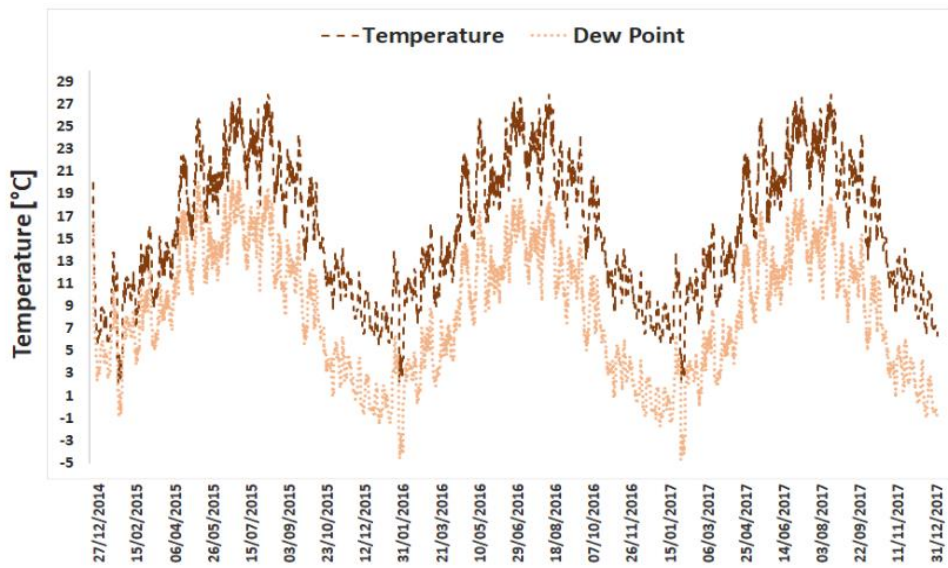


Figure 49: Simulated brick layer temperature and respective dew point temperature over a period of three years for the base model

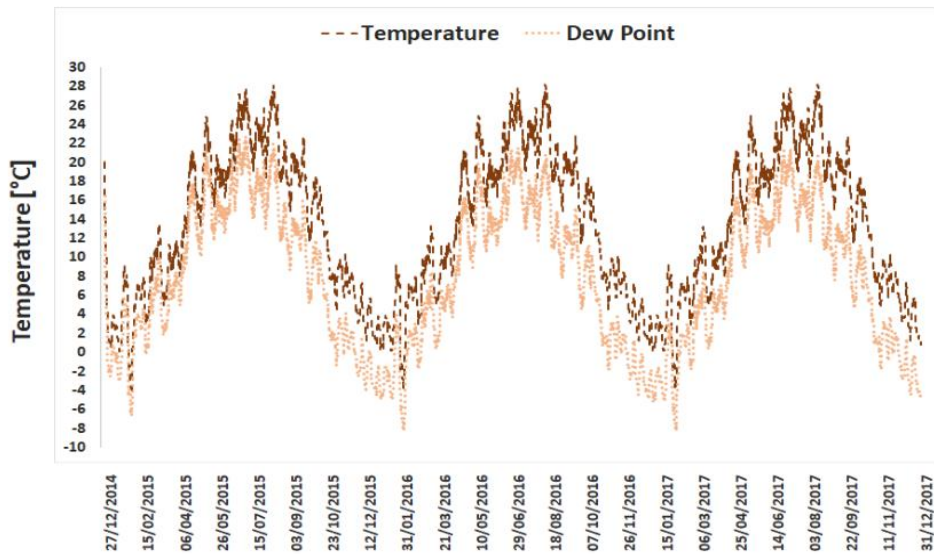


Figure 50: Simulated brick layer temperature and respective dew point temperature over a period of three years for inside position of Aerogel

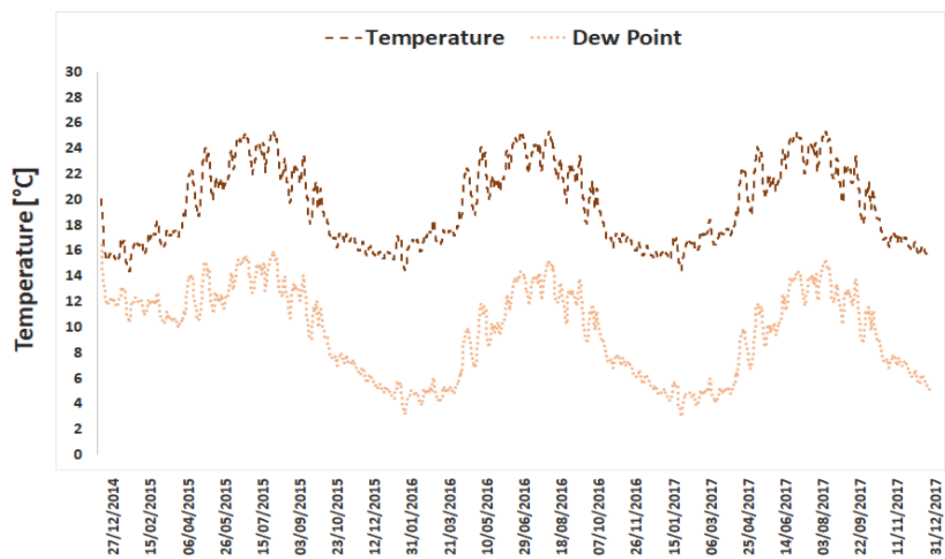


Figure 51: Simulated brick layer temperature and respective dew point temperature over a period of three years for outside position of Aerogel

## CHAPTER 6.

### CONCLUSION

#### 6.1 Contributions

This contribution explored the application of Aerogel plasters to historical building envelopes. The application of such systems has a high impact on the thermal and hygro-thermal performance building components. If properly planned, it is possible to significantly reduce both the building's heating demand and the impact of moisture damages, without compromising the building's architectural appearance. Moreover, it entailed the results of a case study on the predictive performance of hygro-thermal simulations of an existing wall retrofitted with an Aerogel-based plaster layer with different finishing plaster systems in real conditions. The test areas were measured and analyzed over three heating periods. The calculation of an in-situ heat transfer coefficient does not show any significant differences to the one-dimensional calculated value based on the material parameters. With regard to the hygro-thermal behavior, the detailed analysis shows no significant differences between the examined versions of the finishing plaster systems. Measured data was used to both deploy a more accurate initial model and to evaluate the accuracy of the simulation outcome. The results presented the potential of empirically based model calibration for improving simulation tool's predictive performance. Specifically, using local indoor and outdoor climate data, accurate representation of initial conditions, and detailed representation of the building component layers (in this case for hollow brick layer) can yield more reliable simulation results. The study also documented an insulating rendering based on silica Aerogels to be added to the existing external walls without changing the overall appearance. Different insulated wall configurations are studied to compare the thermal and hygro-thermal performance of each one. Results show that interior thermal insulation systems can lead to

moisture problems and condensation risk. The base model, un-insulated wall, has also moisture risks and very high heat losses compared to the other insulated ones. Adding the aerogel-based rendering on the exterior surface of wall reduces significantly or removes the moisture risks. It also reduces considerably the wall heat losses. In terms of thickness evaluation, application of aerogel plaster could reduce annual heating loads from roughly 23% to 36%, depending on the layer thickness.

## **6.2 Future Research**

In author's view the study results have implications beyond the performance comparison of the models considered. Achievement to the optimized thickness of insulation is needed to consider simultaneously other effective parameters, which will deal with in the future study. Comparing the initial material price and payback period of this system with other similar common material, in order to analysis of life cycle assessment could be more generally clarify the importance of utilities such new materials. Moreover, as stressed before, the present study was based on a limited set of data obtained from one office area. Ongoing and future – more extensive – cross-sectional investigations in this area are expected to utilize a larger empirical foundation and thus lead to more representative and inclusive development and evaluation of simultaneously thermal and hygro-thermal behavior models that could be embedded in high.

## CHAPTER 7. REFERENCE

### 7.1 LITERATURE

“(WBCSD) Energy Efficiency in Buildings—Transforming the Market, World Business Council for Sustainable Development, Geneva.” 2009. 2009.

4108, DIN. n.d. “Wärmeschutz Im Hochbau (Insulation in Building Construction).”

Baetens Ruben, Petter Jelle Bjorn, Gustavsen Arild. 2011. “Review: Aerogel Insulation for Building Applications: A State-of-the-Art Review.” *Energy & Buildings* 43: 761–69. <https://doi.org/10.1016/j.enbuild.2010.12.012>.

Beck, A, M Reim, W Körner, and J Fricke. 2002. “Highly Insulating Aerogel Glazing.” *Solar Energy* 72: 21–29.

Berardi, Umberto. 2015. “The Development of a Monolithic Aerogel Glazed Window for an Energy Retrofitting Project.” *Applied Energy* 154: 603–15. <https://doi.org/10.1016/j.apenergy.2015.05.059>.

Buratti, Cinzia, Francesca Merli, and Elisa Moretti. 2017. “Aerogel-Based Materials for Building Applications: Influence of Granule Size on Thermal and Acoustic Performance.” *Energy and Buildings* 152: 472–82. <https://doi.org/10.1016/j.enbuild.2017.07.071>.

Cammerer, J. und Achtziger, J.: Einfluß des. 1985. “Feuchtegehaltes Auf Die Wärmeleitfähigkeit von Bau- Und Dämmstoffen (Effect of the Moisture Content on the Thermal Conductivity of Building Materials and Insulation Products).” *Kurzberichte Aus Der Bauforschung*, Nr. 115, S. 491-494.

Challenge, Recognising The. 2018. “Managing Moisture & Condensation in Buildings Assessment Methodologies - WUFI vs . Glaser - BS5250

Update,” 1–17.

Cuce, Erdem, Pinar Mert Cuce, Christopher J. Wood, and Saffa B. Riffat. 2014. “Toward Aerogel Based Thermal Superinsulation in Buildings: A Comprehensive Review.” *Renewable and Sustainable Energy Reviews* 34: 273–99. <https://doi.org/10.1016/j.rser.2014.03.017>.

Eisenhower, Bryan, Zheng O’Neill, Vladimir A. Fonoberov, and Igor Mezić. 2012. “Uncertainty and Sensitivity Decomposition of Building Energy Models.” *Journal of Building Performance Simulation* 5 (3): 171–84. <https://doi.org/10.1080/19401493.2010.549964>.

El-Darwish, Ingy, and Mohamed Gomaa. 2017. “Retrofitting Strategy for Building Envelopes to Achieve Energy Efficiency.” *Alexandria Engineering Journal* 56 (4): 579–89. <https://doi.org/10.1016/j.aej.2017.05.011>.

European Commission. 2016. *Overview of Support Activities and Projects of the European Union on Energy Efficiency and Renewable Energy in the Heating and Cooling Sector*. Publications Office of the European Union. <https://doi.org/10.2826/607102>.

European Parliament. 2012. “Directive 2012/27/EU of the European Parliament and of the Council of 25 October 2012 on Energy Efficiency.” *Official Journal of the European Union Directive*, no. October: 1–56. [https://doi.org/10.3000/19770677.L\\_2012.315.eng](https://doi.org/10.3000/19770677.L_2012.315.eng).

F. Pacheco Torgal, Cinzia Buratti, Siva Kalaiselvam, Claes-Göran Granqvist, and Volodymyr Ivanov. 2016. *Nano Biotech Based Materials for Energy Building Efficiency*. Switzerland: Springer. <https://doi.org/10.1007/978-3-319-27505-5>.

Fixit. 2018. “Fixit 222.”. *Last Accessed on 10.06.2017*.

Glaser, H. 1985. “Vereinfachte Berechnung Der Dampfdiffusion Durch

Geschichtete Wände Bei Ausscheidung von Wasser Und Eis (Simplified Calculation of Vapour Diffusion through Layered Walls Involving the Formation of Water and Ice). *Kältetechnik* 10, H. 11, S. 358-364 Und H. .”

Hagentoft, Carl-Eric, Angela Sasic Kalagasidis, Bijan Adl-Zarrabi, Staf Roels, Jan Carmeliet, Hugo Hens, John Grunewald, et al. 2004. “Assessment Method of Numerical Prediction Models for Combined Heat, Air and Moisture Transfer in Building Components: Benchmarks for One-Dimensional Cases.” *Journal of Building Physics* 27 (4): 327–52. <https://doi.org/10.1177/1097196304042436>.

“[Http://Www.Aerogel.Org/.](http://www.aerogel.org/)” 2019. Open Source Nanotech. 2019/ *Last Accessed on 10.06.2017*.

[Http://www.buildup.eu/en](http://www.buildup.eu/en). n.d./*Last Accessed on 10.06.2017*.

“[Https://Www.Aerogel.Com/Resources/Health-and-Safety/.](https://www.aerogel.com/resources/health-and-safety/)” 2019/ *Last Accessed on 10.06.2017*.

Ibrahim, Mohamad, Etienne Wurtz, Pascal Henry Biwole, Patrick Achard, and Hebert Sallee. 2014. “Hygrothermal Performance of Exterior Walls Covered with Aerogel-Based Insulating Rendering.” *Energy and Buildings* 84: 241–51. <https://doi.org/10.1016/j.enbuild.2014.07.039>.

ISO 9869. 1994. “Thermal Insulation – Building Elements – In-Situ Measurement of Thermal Resistance and Thermal Transmittance.” *International Organization of Standardization, Geneva, Switzerland, Nternational Standard ISO 9869*.

Itard, L., F. Meijer, E. Vrans, and H. Hoiting. 2008. “Building Renovation and Modernisation in Europe : State of the Art Review. Final Report.” *TU Delft*, no. January.

Kießl, K. und Gertis, K. 1980. "Feuchtetransport in Baustoffen (Moisture Transport in Building Materials)." *Forschungsberichte Aus Dem Fachbereich Bauwesen, H. 13, Universität- Gesamthochschule Essen.*

Kießl, K. 1983. "Kapillarer Und Dampfförmiger Feuchtetransport in Mehrschichtigen Bau- Teilen (Capillary and Vaporous Moisture Transport in Multi-Layered Building Com- Ponents)." *Diss. Universität-Gesamthoch- Schule Essen.*

Kistler, S. S. 1930. "Coherent Expanded Aerogels." *Rubber Chemistry and Technology* 5 (4): 600–603. <https://doi.org/10.5254/1.3539386>.

Kong, Fanhong, and Huaizhu Wang. 2011. "Heat and Mass Coupled Transfer Combined with Freezing Process in Building Materials: Modeling and Experimental Verification." *Energy and Buildings* 43 (10): 2850–59. <https://doi.org/10.1016/j.enbuild.2011.07.004>.

Kosny, J., A. Fallahi, and N. Shukla. 2013. "Cold Climate Building Enclosure Solutions." *Related Information: Work Performed by the Fraunhofer Center for Sustainable Energy Systems, Cambridge, Massachusetts*, no. January. <https://doi.org/10.2172/1068619>.

Krischer, O. und Kast, W. n.d. "Die Wissenschaftlichen Grundlagen Der Trock- Nungstechnik (The Scientific Principles of Drying Technology)." *Dritte Auflage, Springer- Verlag.*

Künzel, Hartwig. 1986. "Bestimmt Der Volumen- Oder Der Massebezogene Feuchtegehalt Die Wärme- Leitfähigkeit von Baustoffen? (Does the Volume-Related or the Mass-Related Moisture Content Determine the Thermal Conductivity of Building Materials?)." *Bauphysik* 8, H. 2, S. 33-39.

Künzel, Hartwig M., and Andreas H. Holm. 2009. "Moisture Control and Problem Analysis of Heritage Construction." *Patorreb*, 85–102. <https://www.ibp.fraunhofer.de/content/dam/ibp/de/documents/P>



ublikationen/Konferenzbeitraege/Englisch/Künzel\_2009\_Moisture-control-problem-analysis-Heritage\_tcm45-86541.pdf.

Künzel, Hartwig M. 1995. *Simultaneous Heat and Moisture Transport in Building Components One- and Two-Dimensional Calculation Using Simple Parameters*. Physics. Vol. 1995. [https://doi.org/10.1016/S0167-4103-8167-4103-7](https://doi.org/10.1016/S0167-4103(95)00007-7).

L. Forest, V. Gibiat, A. Hooley. 2001. "Impedance Matching and Acoustic Absorption in Granular Layers of Silica Aerogels." *J. Non-Cryst. Solids* 285, 230–35.

L. Forest, V. Gibiat, T. Woignier. 1998. "Biots Theory of Acoustic Propagation in Porous Media Applied to Aerogels and Alkogels." *J. Non-Cryst. Solids* 225, 287–92.

M. Reim, W. Körner, J. Manara, S. Korder, M. Arduini-Schuster, H.-P. Ebert, J. Fricke. 2005. "Silica Aerogel Granulate Material for Highly Thermal Insulation and Daylighting." *Solar Energy* 79(2), 131–39.

Masera, Gabriele, Karim Ghazi Wakili, Thomas Stahl, Samuel Brunner, Rosanna Galliano, Carol Monticelli, Stefano Aliprandi, Alessandra Zanelli, and Amr Elesawy. 2017a. "Development of a Super-Insulating, Aerogel-Based Textile Wallpaper for the Indoor Energy Retrofit of Existing Residential Buildings." *Procedia Engineering* 180: 1139–49. <https://doi.org/10.1016/j.proeng.2017.04.274>.

"Development of a Super-Insulating, Aerogel-Based Textile Wallpaper for the Indoor Energy Retrofit of Existing Residential Buildings." *Procedia Engineering* 180 (May): 1139–49. <https://doi.org/10.1016/j.proeng.2017.04.274>.

Meteonorm. 2017. "Meteonorm." [Http://Www.Meteonorm.Com/En/Product/Productpage/Meteonorm-Software/](http://www.meteonorm.com/en/product/productpage/meteonorm-software/). Last Accessed on 10.06.2017.

Mundt Petersen, SOlof, and Lars Erik Harderup. 2013. "Validation of a One-Dimensional Transient Heat and Moisture Calculation Tool under Real Conditions." *Thermal Performance of the Exterior Envelopes of Whole Buildings XII* Sweden: 12.

Nocentini, Kevin, Patrick Achard, and Pascal Biwole. 2018. "Hygro-Thermal Properties of Silica Aerogel Blankets Dried Using Microwave Heating for Building Thermal Insulation." *Energy and Buildings* 158: 14–22.  
<https://doi.org/10.1016/j.enbuild.2017.10.024>.

Ozel, Meral. 2014. "Effect of Insulation Location on Dynamic Heat-Transfer Characteristics of Building External Walls and Optimization of Insulation Thickness." *Energy and Buildings* 72: 288–95.  
<https://doi.org/10.1016/j.enbuild.2013.11.015>.

P. Ricciardi, V. Gibiat, A. Hooley. n.d. "Multilayer Absorbers of Silica Aerogel." *Proc.Forum Acusticum, Sevilla*.

P. Ricciardi, V. Gibiat. n.d. "Acoustic Emissions for Silica Avalanches, in: The 18th International Congress on Acoustics." *ICA 2004, Kyoto, Japan*.

Pannell, David J. 2017. "Sensitivity Analysis : Strategies , Methods , Concepts , Examples," 1–15.

Proskurnina, Olga. n.d. "Application of Aerogel-Based Plaster towards Thermal Retrofit of Historical Facades : A Computational Assessment."

Reddy, T. Agami. 2006. "Literature Review on Calibration of Building Energy Simulation Programs: Uses, Problems, Procedures, Uncertainty, and Tools." *ASHRAE Transactions* 112 (1): 226–40.  
<https://doi.org/Article>.

Santamouris, M., and E. Dascalaki. 2002. "Passive Retrofitting of Office

Buildings to Improve Their Energy Performance and Indoor Environment: The OFFICE Project.” *Building and Environment* 37 (6): 575–78. [https://doi.org/10.1016/S0360-1323\(02\)00004-5](https://doi.org/10.1016/S0360-1323(02)00004-5).

Schuss, Mattias, Ardeshir Mahdavi, Ulrich Pont, Christian Sustr, Samira Aien, Karim Ghazi Wakili, and Thomas Stahl. 2017. “Strukturierte Aerogelputze.” In *Bauphysik-Kalender 2017*, 153–75. Berlin: Ernst&Sohn.Architektur und technische Wissenschaften.

Shukla, Dr. Nitin, Dr. Ali Fallahi, and Dr. Jan Kosny. 2012. “Aerogel for Thermal Insulation of Interior Wall Retrofits in Cold Climates.” *Fraunhofer Center for Sustainable Energy Systems*, 1–11.

Smitha, S., Shajesh, P., Aravind, P. R., Rajesh Kumar, S., Krishna Pillai, P., Warriar, K. G. K. n.d. “Effect of Aging Time and Concentration of Aging Solution on the Porosity Characteristics of Subcritically Dried Silica Aerogels.” *Microporous and Mesoporous Materials* 91 (1–3): 286–92.

Soleimani Dorcheh, A., and M. H. Abbasi. 2008. “Silica Aerogel; Synthesis, Properties and Characterization.” *Journal of Materials Processing Technology* 199 (1): 10–26. <https://doi.org/10.1016/j.jmatprotec.2007.10.060>.

Stahl, Th, S Brunner, M Zimmermann, and K. Ghazi Wakili. 2012. “Thermo-Hygric Properties of a Newly Developed Aerogel Based Insulation Rendering for Both Exterior and Interior Applications.” *Energy and Buildings* 44 (1): 114–17. <https://doi.org/10.1016/j.enbuild.2011.09.041>.

TABULA. 2018. “[Http://Webtool.Building-Typology.Eu/#bm](http://Webtool.Building-Typology.Eu/#bm).”/ *Last Accessed on 10.06.2017*.

Tahmasebi, F, and A Mahdavi. 2013. “A Two-Stage Simulation Model Calibration Approach to Virtual Sensors for Building Performance Data.” *Proceedings of the 13th International Conference of the*

*International Building Performance Simulation Association*, 608–13.  
<http://www.scopus.com/inward/record.url?eid=2-s2.0-84886693964&partnerID=40&md5=de13d23c447959bd4e6eaccde19ff8bc>.

Ürge-Vorsatz, Diana, Luisa F. Cabeza, Susana Serrano, Camila Barreneche, and Ksenia Petrichenko. 2015. “Heating and Cooling Energy Trends and Drivers in Buildings.” *Renewable and Sustainable Energy Reviews* 41: 85–98.  
<https://doi.org/10.1016/j.rser.2014.08.039>.

Wong, I. L., P. C. Eames, and R. S. Perera. 2007. “A Review of Transparent Insulation Systems and the Evaluation of Payback Period for Building Applications.” *Solar Energy* 81 (9): 1058–71.  
<https://doi.org/10.1016/j.solener.2007.04.004>.

WUFI. 2011. “IBP, WUFI® Pro Version 5.1, (<http://www.WUFI.de/Index.e.html>) (15 January 2013).” Germany: Fraunhofer Institute for Building Physics, Holzkirchen/ *Last Accessed on 10.06.2017*.

Xian Yue, Junyong Chen, Huaxin Li, Zhou Xiao, Xianbo Yua and Junhui Xiang. 2020. “One Pot Rapid Synthesis of Ultra High Strength Hydrophobic Bulk Silica Aerogels.” *Material Chemistry Frontiers*, no. 8: 2418–27.

Xin, Liu, Wang Chenchen, Liang Chuanzhi, Feng Guohui, Yin Zekai, and Li Zonghan. 2018. “Effect of the Energy-Saving Retrofit on the Existing Residential Buildings in the Typical City in Northern China.” *Energy and Buildings*. <https://doi.org/10.1016/j.enbuild.2018.07.004>.

## 7.2 List of tables

TABLE 1: POTENTIALS HAZARDOUS EFFECT OF AEROGELS ON HUMAN HEALTH .....	13
TABLE 2: INPUT DATA PERTAIN TO THE THERMAL AND HYGRO-THERMAL PROPERTIES OF MATERIAL .....	29
TABLE 3: COMBINATIONS OF EXTERIOR PLASTER OF FIELDS 1 TO 4 .....	30
TABLE 4: THE PERIOD OF MISSED MEASURED DATA .....	34
TABLE 5: GENERAL SETTING AND INPUT OF WUFI (PRO – 2D) .....	44
TABLE 6: INITIAL CONDITIONS ASSUMPTIONS IN THE INITIAL SIMULATION MODEL .....	45
TABLE 7: VARIABLES SUBJECTED TO SA AND THEIR RANGES VARIABLES .....	50
TABLE 8: SIMULATION SCENARIOS .....	55
TABLE 9: CONSTRUCTION DATA ON AUSTRIA BUILDING TYPES .....	67
TABLE 10: <i>RETROFIT SCENARIOS</i> .....	71
TABLE 11: ANNUAL HEATING AND COOLING REDUCTION (AS COMPARED TO THE BASE MODEL) FOR VARIOUS INSULATION THICKNESS VALUES (SCENARIOS A1, B1, C1, AND D1) .....	73

### 7.3 List of equations

$H_s = P_s C_s \theta$	EQ. 1	.....	19
$\Lambda(W) = \Lambda_0(1 + B \cdot W / P_s)$	EQ. 2	.....	20
$F \text{ VALUE} = \theta X, Y - \theta E \theta I - \theta E$	EQ. 3	.....	39
$\Omega = 0.622 \Phi \cdot P_G P_A$	EQ. 4	.....	39
WITH $P_A = P - P_V$ AND $P_V = \Phi \cdot P_G$	EQ. 5	.....	39
$P_G = 611.2 \times \text{EXP}(17.62 \times T / 243.12 + T)$	EQ. 6	.....	39
$\theta_{DP} = RH1000.125.112 + 0.9\theta_{AIR} + 0.1\theta_{AIR} - 112 \text{ } ^\circ\text{C}$	EQ. 7	.....	44
$W_i - W_1 = W_2 - W_1 RH_2 - RH_1 \cdot RH_i - RH_1$	EQ. 8	.....	45
$E_{ABSOLUTE} = MI - SI$	EQ. 9	.....	47
$E_{RELATIVE} = MI - SIMI$	EQ. 10	.....	47
$RMSD = I = 1 NMI - SI^2 N$	EQ. 11	.....	48
$CVRMSD = RMSD M. 100$	EQ. 12	.....	48
$R^2 = NMISI - MISI(NMI^2 - MI^2) \cdot (NSI^2 - SI^2)^2$	EQ. 13	.....	48

## 7.4 List of figures

FIGURE 1: STRUCTURE OF SILICA AEROGEL (XIAN YUE, JUNYONG CHEN, HUAXIN LI, ZHOU XIAO 2020) .....	10
FIGURE 2: EXAMPLES OF TRANSLUCENT SILICA AEROGEL INSULATION BLOCK FORM (BERARDI 2015) .....	15
FIGURE 3: SAMPLE OF THE MONOLITHIC AEROGEL PANEL USED IN THE GLAZING UNITS (BERARDI 2015) .....	15
FIGURE 4: GRANULAR FILLED AEROGEL WINDOWS: DETROIT SCHOOL OF ARTS, MI, USA (BERARDI 2015) .....	15
FIGURE 5: GRANULAR FILLED AEROGEL WINDOWS: NOBEL HALLS AT SUNY STONY BROOK, NY, USA APPLIED OVER LARGE AREAS IN NEW BUILDINGS FOR DAY LIGHTING PURPOSES (BERARDI 2015) .....	16
FIGURE 6: RENDERING FIXIT 222 WITH AEROGEL (PROSKURNINA, N.D.) .....	16
FIGURE 7: CROSS-SECTION THROUGH THE GRANULAR AEROGEL BASED GLAZING, CONSISTING OF TWO GLASS PANELS WITH A LOW-E COATING ON THE INSIDE, TWO GAPS AND AN AEROGEL-FILLED PMMA DOUBLE-SKIN-SHEET DOUBLE-SKIN-SHEET (M. REIM, W. KÖRNER, J. MANARA, S. KORDER, M. ARDUINI-SCHUSTER, H.-P. EBERT 2005) .....	17
FIGURE 8: VIEW OF THE TEST AREAS ON THE SOUTH FAÇADE (FIELDS 1-4), WEST FAÇADE (FIELDS 5-8), AND NORTH FAÇADE (FIELDS 9-10) (SCHUSS ET AL. 2017) .....	27
FIGURE 9: THE LAYER SECTION OF TESTED FACADE .....	28
FIGURE 10: THE SOUTH TESTED SURFACE, WHICH HAS DIVIDED FOUR FIELDS (SCHUSS ET AL. 2017) .....	29
FIGURE 11: ADHESIVE PRIMER (ON THE LEFT), APPLICATION OF FIXIT 222 WITH A PLASTERING MACHINE (ON THE RIGHT) (PROSKURNINA, N.D.) .....	30
FIGURE 12: LEVELLING OFF FIXIT 222(LEFT), SURFACE OF FIXIT 222(RIGHT) (PROSKURNINA, N.D.) .....	31
FIGURE 13: REINFORCEMENT MESH FOR CORNERS OF OPENING (LEFT), APPLICATION OF REINFORCEMENT MESH (RIGHT) (PROSKURNINA, N.D.) .....	31
FIGURE 14: APPLIED REINFORCEMENT MESH (LEFT), FIXIT 222 INSULATION PLASTER (RIGHT) (PROSKURNINA, N.D.) .....	32
FIGURE 15: VIEW OF SENSORS BEFORE THE APPLICATION OF THE AEROSOL PLASTER AND THE POSITION OF SENSORS IN THE LAYERS OF CONSTRUCTION IN SOUTH ORIENTATION (SCHUSS ET AL. 2017) .....	33
FIGURE 16: THE SOLAR RADIATION AND TEMPERATURE / HUMIDITY SENSORS (SCHUSS ET AL. 2017) .....	33



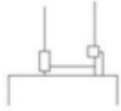

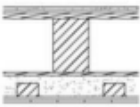
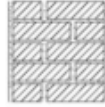
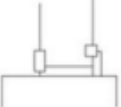

FIGURE 17: HEAT FLOW-WINTER PERIOD 2013/2014 .....	35
FIGURE 18: HEAT FLOW-WINTER PERIOD 2014/2015 .....	35
FIGURE 19: HEAT FLOW-WINTER PERIOD 2015/2016 .....	35
FIGURE 20: DISTRIBUTION MEASURED TEMPERATURE AND RELATIVE HUMIDITY IN ALL POSITIONS OF TEST AREAS / YEAR 2015 .....	37
FIGURE 21: DISTRIBUTION MEASURED TEMPERATURE AND RELATIVE HUMIDITY IN ALL POSITIONS OF TEST AREAS / HEATING PERIOD 2015 .....	38
FIGURE 22: DISTRIBUTION CALCULATED F-VALUE AND SPECIFIC HUMIDITY IN ALL POSITIONS OF TEST AREAS / YEAR 2015 .....	40
FIGURE 23: DISTRIBUTION CALCULATED F-VALUE AND SPECIFIC HUMIDITY IN ALL POSITIONS OF TEST AREAS / HEATING PERIOD 2015 .....	41
FIGURE 24: LAYER'S GEOMETRY MODELLED IN WUFI PRO (LEFT) AND IN WUFI 2D (RIGHT). .....	43
FIGURE 25: THE MONITOR POSITIONS OF EACH NODE ACCORDING TO THE REAL CONDITION ..	45
FIGURE 26: AEROGEL- BASED RENDERING SORPTION CURVE (IBRAHIM ET AL. 2014) .....	46
FIGURE 27: R <sup>2</sup> –VALUE OF TEMPERATURE OF ANALYSED VARIABLES .....	51
FIGURE 28: R <sup>2</sup> –VALUE OF RELATIVE HUMIDITY OF ANALYSED VARIABLES .....	51
FIGURE 29: RMSD –VALUE OF TEMPERATURE OF ANALYSED VARIABLES .....	52
FIGURE 30: RMSD –VALUE OF RELATIVE HUMIDITY OF ANALYSED VARIABLES .....	52
FIGURE 31: (CV) RMSD –VALUE OF TEMPERATURE OF ANALYSED VARIABLES .....	53
FIGURE 32: (CV) RMSD –VALUE OF RELATIVE HUMIDITY OF ANALYSED VARIABLES .....	53
FIGURE 33: LAYER'S GEOMETRY MODELLED IN 2D (LEFT), AND WUFI PRO (RIGHT) .....	56
FIGURE 34: DISTRIBUTION MEASURED RELATIVE HUMIDITY IN ALL SCENARIOS AND EACH NODE .....	57
FIGURE 35: DISTRIBUTION MEASURED TEMPERATURE IN ALL SCENARIOS AND EACH NODE .....	57
FIGURE 36: R <sup>2</sup> OF RELATIVE HUMIDITY (LEFT) AND TEMPERATURE (RIGHT) OF ALL SCENARIOS IN EACH NODE.....	59
FIGURE 37: (CV) RMSD OF RELATIVE HUMIDITY (LEFT) AND TEMPERATURE (RIGHT) OF ALL SCENARIOS IN EACH NODE.....	60
FIGURE 38: ABSOLUTE ERROR OF RELATIVE HUMIDITY [%] OF ALL SCENARIOS FOR EACH NODE .....	62
FIGURE 39: ABSOLUTE ERROR OF TEMPERATURE [K] OF ALL SCENARIOS FOR EACH NODE .....	62
FIGURE 40: RELATIVE ERROR OF RELATIVE HUMIDITY OF EXTERIOR PLASTER .....	63
FIGURE 41: RELATIVE ERROR OF RELATIVE HUMIDITY OF AEROGEL LAYER .....	63
FIGURE 42: RELATIVE ERROR OF RELATIVE HUMIDITY OF BRICK LAYER .....	64
FIGURE 43: RELATIVE ERROR OF RELATIVE HUMIDITY OF INTERIOR PLASTER .....	64

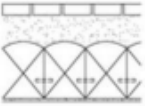

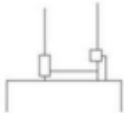

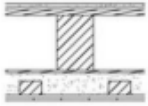

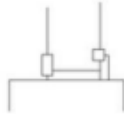



FIGURE 44: TREND OF RELATIVE HUMIDITY IN MIDDLE OF THE WALL-BRICK LAYER .....65  
 FIGURE 45: PLAN AND SECTION THERMAL ZONING OF THE CASE STUDY BUILDING MODEL .....68  
 FIGURE 46: 3D MODELLING IN SKETCH UP- OPEN STUDIO TO IMPORT TO ENERGY-PULSE  
 SOFTWARE.....70  
 FIGURE 47: COMPARISON OF THE SIMULATED SCENARIOS (SEE TABLE 10) IN TERMS OF THE  
 RESULTING MONTHLY HEATING LOADS (MONTHS WITHOUT HEATING LOAD ARE  
 EXCLUDED) .....72  
 FIGURE 48: SIMULATED WHOLE CONSTRUCTION WATER CONTENT OVER A PERIOD OF THREE  
 YEARS FOR DIFFERENT CONFIGURATIONS.....73  
 FIGURE 49: SIMULATED BRICK LAYER TEMPERATURE AND RESPECTIVE DEW POINT  
 TEMPERATURE OVER A PERIOD OF THREE YEARS FOR THE BASE MODEL .....74  
 FIGURE 50: SIMULATED BRICK LAYER TEMPERATURE AND RESPECTIVE DEW POINT  
 TEMPERATURE OVER A PERIOD OF THREE YEARS FOR INSIDE POSITION OF AEROGEL .....74  
 FIGURE 51: SIMULATED BRICK LAYER TEMPERATURE AND RESPECTIVE DEW POINT  
 TEMPERATURE OVER A PERIOD OF THREE YEARS FOR OUTSIDE POSITION OF AEROGEL ...75

## 7.5 Building Matrix

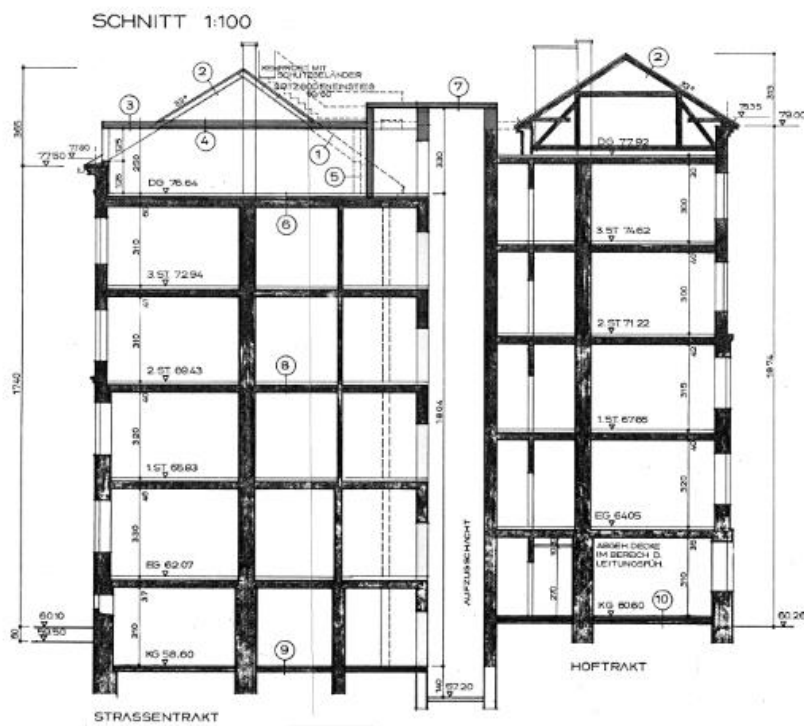
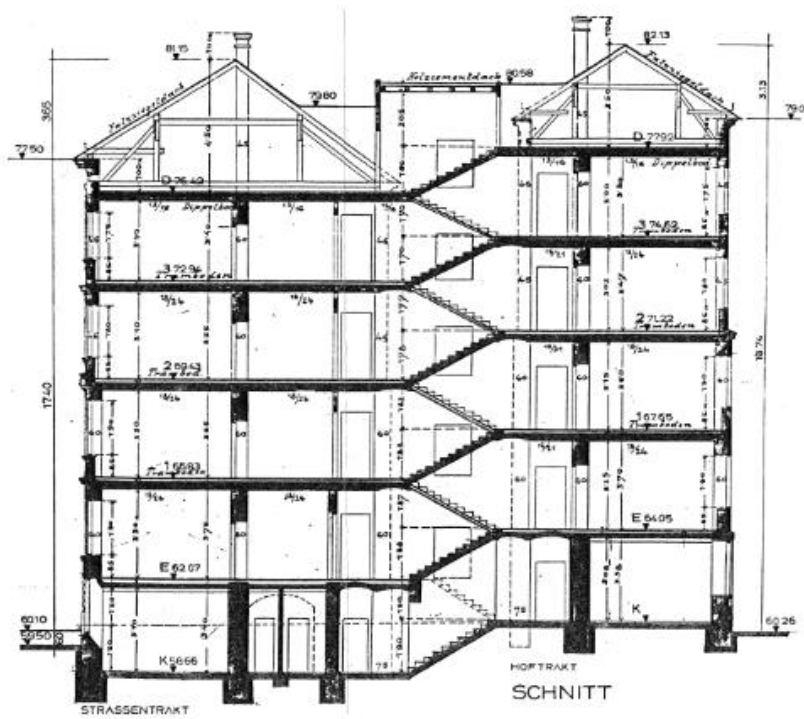
Construction data on Austrian building types (TABULA project)

	Roof	Wall	Window	Floor
SFH (single-family house) Construction time till 1919				
	$U=1.4 \text{ W}\cdot\text{m}^{-2}\cdot\text{K}^{-1}$	$U=1.1 \text{ W}\cdot\text{m}^{-2}\cdot\text{K}^{-1}$	$U=2.2 \text{ W}\cdot\text{m}^{-2}\cdot\text{K}^{-1}$	$U=1.6 \text{ W}\cdot\text{m}^{-2}\cdot\text{K}^{-1}$
	tilted wooden roof, plastered, clay tile	solid brick wall	single glazing box-type windows	concrete ceiling
TH (terraced house) Construction time till 1919				
	$U=0.8 \text{ W}\cdot\text{m}^{-2}\cdot\text{K}^{-1}$	$U=1.1 \text{ W}\cdot\text{m}^{-2}\cdot\text{K}^{-1}$	$U=2.2 \text{ W}\cdot\text{m}^{-2}\cdot\text{K}^{-1}$	$U=0.71 \text{ W}\cdot\text{m}^{-2}\cdot\text{K}^{-1}$
	wooden ceiling with filling, wooden planks	solid brick wall	single glazing box-type windows	brick vault ceiling

<b>MFH (multi-family house)</b>  <b>Construction time till 1919</b>				
	$U=1.95 \text{ W}\cdot\text{m}^{-2}\cdot\text{K}^{-1}$	$U=1.1 \text{ W}\cdot\text{m}^{-2}\cdot\text{K}^{-1}$	$U=2.2 \text{ W}\cdot\text{m}^{-2}\cdot\text{K}^{-1}$	$U=1.08 \text{ W}\cdot\text{m}^{-2}\cdot\text{K}^{-1}$
	wooden anchor beam ceiling with filling, wooden planks`	solid brick wall	single glazing box-type windows	Concrete ceiling
<b>AB (apartment block)</b>  <b>Construction time till 1919</b>				
	$U=0.8 \text{ W}\cdot\text{m}^{-2}\cdot\text{K}^{-1}$	$U=1.1 \text{ W}\cdot\text{m}^{-2}\cdot\text{K}^{-1}$	$U=2.2 \text{ W}\cdot\text{m}^{-2}\cdot\text{K}^{-1}$	$U=0.71 \text{ W}\cdot\text{m}^{-2}\cdot\text{K}^{-1}$
	wooden ceiling with filling, wooden planks	solid brick wall	single glazing box-type windows	brick vault ceiling

## 7.6 Documentation of a building in Habichergasse 20, Vienna

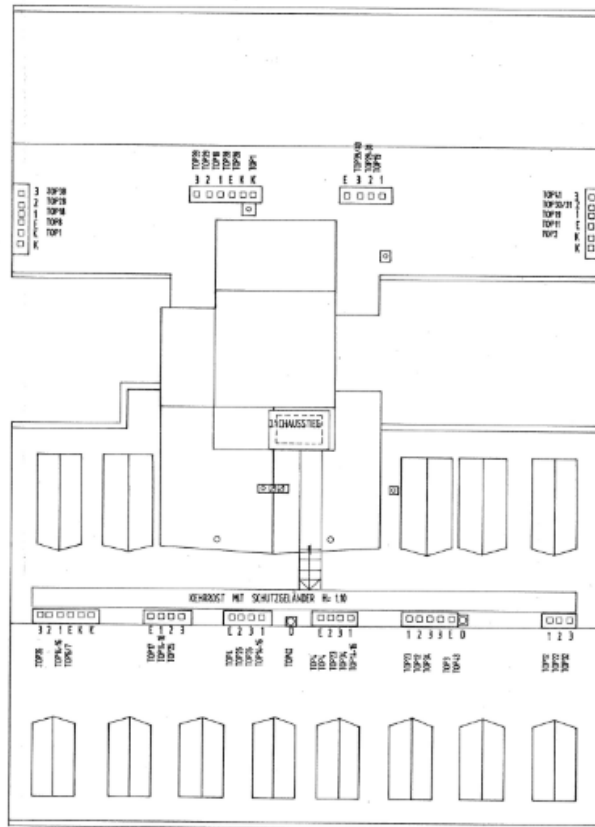
### 7.6.1 Vertical sections of a building in Habichergasse 20, Vienna



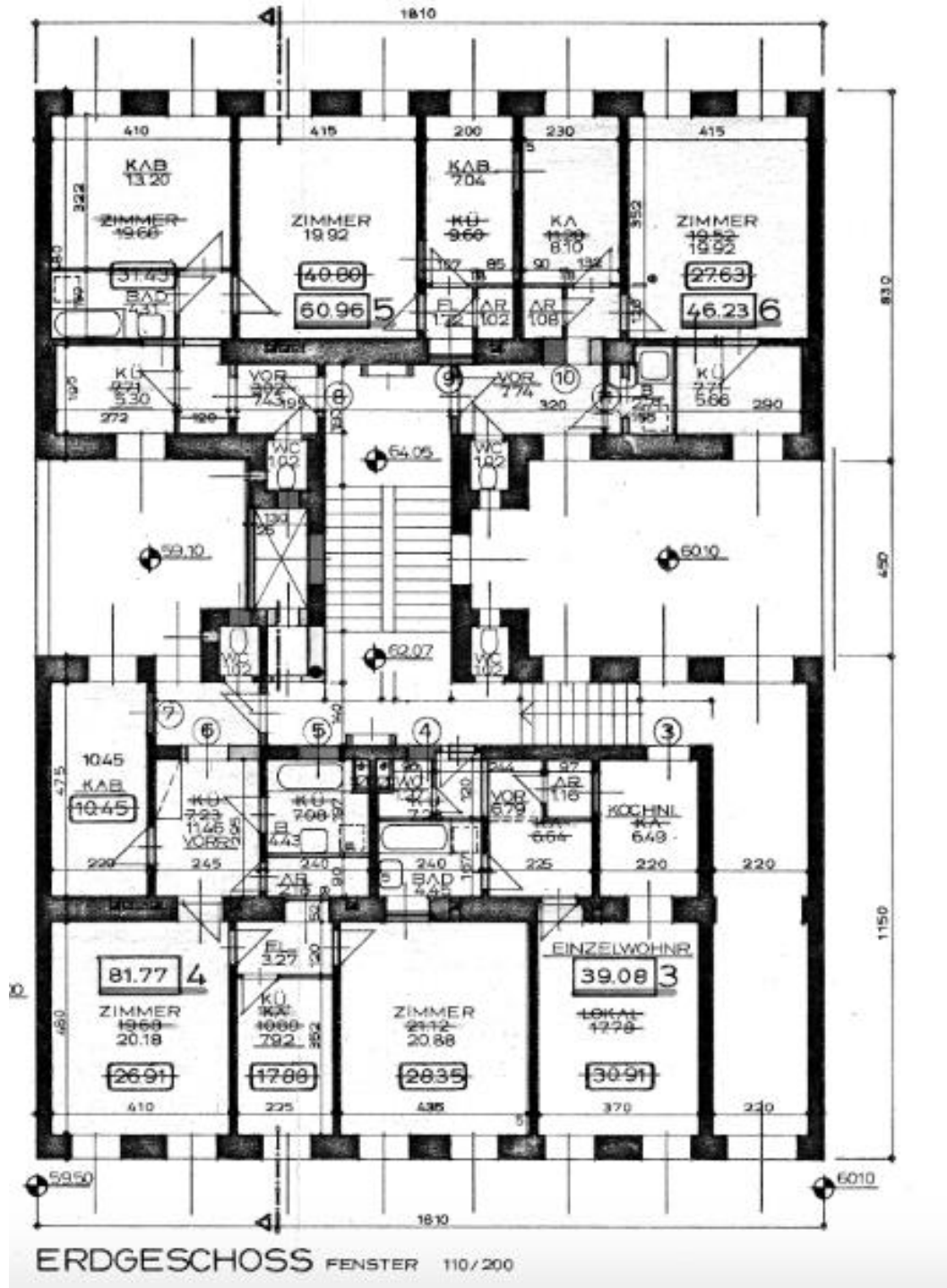
### 7.6.2 Facades of a building in Habichergasse 20, Vienna



### 7.6.3 Roof plan of a building in Habichergasse 20, Vienna



7.6.4 Plan of the first floor of a building in Habichergasse 20, Vienna



# RESUME

Samira Aien

📍 Bach Str.5 13, 89073 Ulm, Germany

☎ +49-17660020518

✉ samiraaien.net@gmail.com

Date of birth 1 Jul 1984 | Nationality Iranian



## Building Physics Engineer - Architecture

### EDUCATION

March 2016–Present P.H.D Candidate

TU Wien, Vienna (Austria)

<https://www.tuwien.ac.at/en/>

- Department of Building Physics and Building Ecology

#### Title of the course

Thermal aspects of building performance, Elements of Building Construction (Aspekte der Hochbaukonstruktion), Visual aspects of building performance, Thermal building performance simulation, Building Ecology

**Title of Thesis:** Thermal and hygro- Thermal performance evaluation of Aerogel containing plaster for retrofit of historic buildings façades : Evaluation of optimum thickness and position of aerogel in layer of construction

Sep 2011–Sep 2013 Master - Sustainable Architecture -Building physics

Ilam University, Ilam (Iran)

<https://www.ilam.ac.ir/en/>

**Title of Thesis:** Study On Effect Of Gypsum Board Containing A Phase Change Material (PCM) In Thermal Performance Of High Inertia Building

Sep 2002–Apr 2007 Bachelor - Architecture

Razi University, Kermanshah (Iran)

<http://www.razi.ac.ir/>

**Title of Thesis:** Design of tourist and accommodation complex (5 star hotel)

## TEACHING

---

- Jul 2013–Nov 2014 Shahid Beheshti University - *Tehran (Iran)*  
- Courses: Drawing and Architecture Design
- Oct 2012–Sep 2014 Azad University of Zarandieh - *Tehran (Iran)*  
- Courses:  
New construction technologies , Introduction to Contemporary Architecture  
WestIndustrial production of buildings , Introduction to Islamic Architecture  
Architecture Design

## EXPERIENCE

---

- Oct 2019- to now Ingenieurbüro für Bauphysik - Ferdinand Ziegler / *Ulm- Aalen (Germany)*  
- Als stellvertretende Geschäftsführerin
- Oct 2018 – Nov 2018 Bauphysik team Zwißlinger und Staffl Engineering OG / *salzburg (Austria)*  
- Thermal simulation  
- hygro/thermal simulation (Moisture transfer)
- Jun 2014 – Sep 2015 PANAM Consultant of Sustainable Design / *Tehran (Iran)*  
- Sustainable Architectural Designing  
- Renovation of existing Buildings  
- Energy simulation Model
- May 2012–Dec 2013 HAFT BANA Consultant of Architectural Design / *Tehran (Iran)*  
- Architectural Design Interior and Exterior  
- Execute of Designed Building  
- Professional in Hospital and Clinic Design
- Jul 2011–Mar 2012 Consultant of Architectural Design / *Tehran (Iran)*  
- Architectural Design Interior and Exterior  
- Execute of Designed Building  
- Researching about Saving Energy In Buildings
- Sep 2008–Apr 2011 Imen Sazan Mandegar Building Company / *Tehran (Iran)*  
- Execute of Designed Building



## IT SKIL

General	Microsoft Office	Advanced
	Photo shop	Advanced
	MATLAB Programming	Intermediate
Architectural	Auto cad 2d&3D	Advanced
	3ds Max	Intermediate
	Sketch up	Advanced
	Revit Architecture	Intermediate
	Archicad	Intermediate
Energy Analyses	Energy plus	Advanced
	Open studio	Advanced
	Design Builder	Advanced
	WUFIPro & WUFI 2D	Advanced
	Archiphysik	Advanced
	LBNL: Therm, Window	Advanced
	Dialux	Intermediate
	PCM Express	Advanced
	Dämmwerk	Advanced
	Soundplan	Advanced

## LANGUAGES

Native Speaker	Persian- Farsi	Other Languages	English
	Azerbaijani		German
			Turkish

# PUBLICATIONS

---

## Publications in Scientific Journals

S. Aien, M. Taheri, S. Pinich, M. Schuss, A. Mahdavi: "**Predictive Performance of Hygro-Thermal Simulation Models: A Case Study**"; Applied Mechanics and Materials, 12th Envibuild - Buildings and Environment - From Research to Application Proceedings of the 12th International EnviBUILD Conference (7th & 8th September 2017) (2019), 887; 401- 408.

## Contributions to Books

M. Schuss, A. Mahdavi, U. Pont, C. Sustr, S. Aien, K. Ghazi Wakili, T. Stahl: "**Strukturierte Aerogelputze**"; in: "Bauphysik-Kalender 2017", 1; N.A. Fouad (ed.); Ernst & Sohn. Verlag für Architektur und technische Wissenschaften Berlin, Berlin, 2017, (invited), ISBN: 9783433031698, 153 - 175.

## Talks and Presentations (with Proceedings-Entry)

S. Aien and A. Mahdavi: "**Hygro-thermal implications of the aerogel-based façade insulation layer position and thickness.**" Talk: IBPSA 2019, Rome, Italy; 2019-09-02 -2019-09-04; in: " Proceedings of the 16th International Building Performance Simulation Association Conference (IBPSA) Conference Rome".

S. Aien, M. Taheri, M. Schuss, and A. Mahdavi: "**A comparison of measured and simulated hygro-thermal performance indicators' values: The case of a retrofitted wall construction.**" Talk: BauSIM2018 - 7. Deutsch-Österreichische IBPSA -Konferenz Tagungsband, Karlsruhe, Germany; 2018-09-26 -2018-09-28; in: "Proceedings of BauSim2018", A. Wagner, P. von Both et al. (ed.); (2018), Paper ID 1117, 7 pages. Abstracts, (2018), ISBN: 978-3-9504017-8-3; 68 - 69.

S. Aien, M. Taheri, A. Mahdavi: "**Performance Evaluation of Various Finishing Layers for Aerogel Plasters**"; Talk: VSS VIENNA young SCIENTISTS SYMPOSIUM, TU Wien; 2018-06-07 - 2018-06-08; in: "VSS -

Venna young scientists symposium", P. Hans, G. Artner, J. Grames, H. Krebs, H. Mansouri Khosravi, T. Rouhi (ed.); Book-of- Abstracts, (2018), ISBN: 978-3-9504017-8-3; 74 - 75.

S. Aien, M. Kordjamshidi, H. Pourfallah: "An **Investigation on Thermal Performance of Rocky Architecture Approaching Thermal Comfort with Less Energy Load**"; Talk: VSS VIENNA young SCIENTISTS SYMPOSIUM, At: Lima, Perú; 2012-11; in: "PLEA2012 - 28th Conference, Opportunities, Limits & Needs Towards an environmentally responsible architecture.